Fakultät für Medizin

Institut für Humangenetik und Neurologische Klinik und Poliklinik

Functional analysis of the RLS-associated *MEIS1* intronic locus

Maria Kaffe

Vollständiger Abdruck der von der Fakultät für Medizin der Technischen Universität München zur Erlangung des akademischen Grades eines

Doctor of Philosophy (Ph.D.)

genehmigten Dissertation.

Vorsitzender: Univ.-Prof. Dr. Florian R. Greten

Prüfer der Dissertation:

1. Univ.-Prof. Dr. Bernhard Hemmer

2. Univ.-Prof. Dr. Thomas A. Meitinger

Die Dissertation wurde am 05.02.2013 bei der Fakultät für Medizin der Technischen Universität München eingereicht und durch die Fakultät für Medizin am 11.03.2013 angenommen.

TABLE OF CONTENTS

ABBREVIATIONS

5’ UTR	5’ untranslated region
BP	Binding potential
bp	Base pairs
BTB domain	Bric-à-brac, tramtrack and broad domain
BTBD9	BTB domain containing 9
ChIP	Chromatin immunoprecipitation
CNS	Central nervous system
CRE	cAMP-responsive element
Creb1	cAMP responsive element binding protein 1
Crem	cAMP responsive element modulatory protein
CSD	“Cold shock” domains
CSF	Cerebrospinal fluid
D2R	Dopamine receptor 2
DA	Dopamine
DAT	Dopamine transporter
Dmbx1	Diencephalon/mesencephalon homeobox 1
DMT1	Divalent metal transporter 1
E	Embryonic day
EMSA	Electrophoretic mobility shift assay
ENCODE	Encyclopedia of DNA Elements
ESRD	End stage renal disease
GWAS	Genome wide association study
HCNR	Highly conserved non-coding region
Kb	Kilobases
LD	Linkage disequilibrium
LGE	Lateral ganglionic eminence
MAP2K5	Mitogen-activated protein kinase 5
MEIS1	Meis homeobox 1
MRI	Magnetic resonance imaging
MZ	Mantle zone

Otx3	Orthodenticle homeobox 3
PET	Positron emission tomography
PLM	Periodic leg movements
PLMS	Periodic leg movements in sleep
PLMW	Periodic leg movements in wakefulness
PTPRD	Protein tyrosine phosphatase, receptor type D
RLS	Restless leg syndrome
RLU	Relative luciferase units
Seq	Sequencing
SKOR1	SKI family transcriptional corepressor 1
SN	Substantia Nigra
SNP	Single nucleotide polymorphisms
SPECT	Single-photon emission computed tomography
TH	Tyrosine hydroxylase
TOX3	TOX high mobility group box family member 3
TSC	Transcranial ultrasound
Ybx1	Y-box binding protein 1

1 INTRODUCTION

1.1 Restless legs syndrome

Restless Legs Syndrome (RLS) is a common and distressing sensorimotor and sleep disorder, with an age-dependent prevalence in the Caucasian population up to 10%, after the age of 65 (Lavigne et al., 1994; Phillips et al., 2000; Allen et al., 2003b; Berger et al., 2004; Hogl et al., 2005). It is clinically diagnosed according to four main criteria formulated by the international RLS study group: an irresistible urge to move the legs and/or unpleasant leg sensations (sometimes the arms or other body parts are also involved); induction or exacerbation of the symptoms at rest; improvement with movement; circadian fluctuations of the symptoms with worsening at the evening and during night (Walters, 1995; Allen et al., 2003a). Up to 80% of RLS patients experience periodic leg movements (PLM) in sleep (PLMS) or awake (PLMW) (Michaud et al., 2002). PLMS are defined as movements lasting more than 500 msec with amplitude of at least 25% of the calibration amplitude and an inter-movement interval of 4-90 sec, which happen in a series of at least four consecutive movements (Coleman et al., 1982; Zucconi et al., 2006). These repetitive movements are associated with an arousal and cause sleep disruption and deprivation (Montplaisir et al., 1997; Allen et al., 2003b; Hening, 2004; Hornyak et al., 2007). As there is at the moment no biomarker for the diagnosis of RLS, the presence of PLMS and a positive family history constitute supportive criteria that further strengthen the diagnosis (Benes et al., 2009). Sympathetic overactivity is associated with RLS/PLMS, as a result of increased pulse rate and blood pressure that coincides with PLMS (Ancoli-Israel et al., 1986; Ware et al., 1988). Thus, there is evidence that highlight a close relationship of RLS/PLMS with

daytime hypertension, cardiovascular and cerebrovascular disease (Walters, 1995; Phillips et al., 2006; Winkelman et al., 2006; Winkelman et al., 2008; Walters et al., 2009).

RLS is a lifelong disorder with progressive symptoms that worsen with age. Idiopathic RLS appears as a stand-alone entity and can be divided in early-onset and late-onset RLS (Ondo et al., 1996; Montplaisir et al., 1997; Winkelmann et al., 2000; Bassetti et al., 2001; Allen et al., 2002; Hanson et al., 2004). Early-onset RLS is usually familial, with an earlier age at onset (before the age of 45 years) and slower progression (Allen et al., 2000; Winkelmann et al., 2002). In contrast, late-onset RLS occurs less commonly in families and progresses rapidly with age (Allen et al., 2000). Secondary RLS is associated with several conditions such as iron deficiency, end stage renal disease, pregnancy, and polyneuropathy, and is also marked with a rapid progression (Trenkwalder et al., 2005).

About 30% of affected individuals have clinically significant RLS and require treatment. Dopaminergic agents are considered as the first-line pharmacological treatment for RLS, with an unknown mechanism of action (Allen et al., 2003b). Patients with low serum ferritin levels can benefit from iron supplementation (Trenkwalder et al., 2008). Additional or alternative treatments include opioids, when dopaminergic agents have no success and anticonvulsants, especially when the symptoms are painful (Walters et al., 2001; Garcia-Borreguero et al., 2002; Sommer et al., 2007).

1.2 Restless legs syndrome pathophysiology

RLS pathophysiology remains to be unraveled. As RLS has both a sensory and motor component, many structures and factors that are involved in somatosensory processing

and generation-coordination of movement seem to be implicated in the pathophysiology of RLS. The notable efficacy of the dopaminergics in alleviating RLS symptoms reinforces a possible role of the dopaminergic neurotransmission in RLS. Iron deficiency both in the periphery and brain has also been associated with RLS, perplexing the theories about RLS pathophysiology (Earley et al., 2000). Some researchers postulate that RLS is a neurological disorder affecting the peripheral nervous system, but the majority describes pathology of the central nervous system (Schattschneider et al., 2004). In addition, the fact that there is a group of patients that is difficult to treat with dopaminergics and profits from the use of opioids or antiepilectics indicate another possible mechanism causing RLS. Last but not least, genetics play a definitive role in RLS, which will be described in detail below.

1.2.1 Dopamine

For the first time, a clear indication of dopamine pathology in RLS was revealed in an autopsy study. This study demonstrated a decrease of the dopamine receptor 2 (D2R) in putamen of RLS patients that correlated also with the severity of RLS (Connor et al., 2009). The phosphorylated (active) tyrosine hydroxylase (TH) was significantly increased in both substantia nigra (SN) and putamen. Significant increase in TH has also been demonstrated in *in-vivo* (rat) and *in-vitro* (PC12 cell line) iron deprivation models similar to that from the RLS autopsy data. This data are consistent with the hypothesis that a primary iron insufficiency dysregulates the dopaminergic metabolism as part of the RLS pathology. It is important to note that iron is a co-factor in the rate-limiting step of the conversion of tyrosine to L-Dopa, which is subsequently

decarboxylated to form dopamine (DA) (Ramsey et al., 1996). Thus, iron and dopamine metabolism are in close relationship in the brain.

Another study assessed in real-time dopamine transporter (DAT) binding potentials (BP) in striatum of RLS patients using positron emission tomography (PET) techniques. RLS subjects showed significantly lower DAT binding in the striatum (putamen and caudate) compared to controls, reinforcing the results of the previous study (Earley et al., 2011). DAT BP did not correlate with any clinical measures of RLS and showed no diurnal differences.

Several previous neuroimaging studies using single-photon emission computed tomography (SPECT) and PET examined both presynaptic and postsynaptic DAT as well as postsynaptic D2R binding to the striatum. Striatal presynaptic DAT have shown no difference between RLS and control group (Eisensehr et al., 2001; Michaud et al., 2002; Linke et al., 2004). Postsynaptically, some SPECT studies failed to find any significant differences for postsynaptic D2-receptor binding (Eisensehr et al., 2001; Tribl et al., 2004), but some others demonstrated a reduction of D2 receptor occupancy in the striatum of RLS patients (Staedt et al., 1993; Staedt et al., 1995; Staedt et al., 1995; Michaud et al., 2002; Tribl et al., 2004). At last, another study also gave evidence for hypoactive dopaminergic neurotransmission in the pathophysiology of RLS (Cervenka et al., 2006). The study supported that extrastriatal (thalamus, insula and anterior cingulate cortex) as well as striatal brain regions are involved. The anterior cingulate cortex is part of the nociceptive system responsible for the effective and emotional component of pain, suggesting a possible pathway for the sensory symptoms of RLS.

1.2.2 Iron

As previously mentioned dopamine synthesis and iron are closely linked to each other, as iron is important for the synthesis of dopamine. Decreased iron levels can elicit or worsen RLS symptoms and iron supplementation helps to resolve these symptoms (Silber et al., 2003; Earley et al., 2005).

The first neuropathological examination of RLS brains showed iron deficiency and more specificaly a decrease in staining for iron and H-ferritin (H-ft) in SN, as well as a decrease in staining for the metal transporter 1 (MTP) and the divalent metal transporter 1 (DMT1) (Connor et al., 2003). The study also demonstrated a deficiency of the iron regulatory protein 1 (IRP1) (Connor et al., 2004). This protein regulates post-transcriptionally the expression of the transferrin receptor (TfR). Its levels and activity were reduced in the RLS samples, implicating a possible mechanism for the iron insufficiency. Furthermore, human SN and putamen autopsy samples were examined and showed increased mitochondrial ferritin levels for the RLS SN samples and no difference for the putamen samples (Snyder et al., 2009). The authors demonstrated an increase in the mitochondria number of RLS SN samples and suggested that these neurons attempt to correct a metabolic insufficiency that may lead to cytosolic iron deficiency.

The main drawback of most of these studies is the prior dopaminergic treatment of RLS patients that can be responsible for some of the pathological features in autopsy samples. In addition, the same biopsy tissue has been used in many studies. The reproducibility with independent samples/investigators and with no previous medication, will clarify any uncertainty about the reliability of these outcomes.

The first magnetic resonance imaging (MRI) study, measuring brain iron in RLS patients, demonstrated a decrease of iron in the SN and a marginally but not significant decrease in putamen, both positively correlated with RLS severity (Allen et al., 2001). Furthermore, transcranial ultrasound (TSC) also supported the hypothesis of nigral iron deficiency in RLS patients (Schmidauer et al., 2005; Godau et al., 2007). Another study employing T2 relaxometry demonstrated the same and a tendency towards lower iron content in caudate and dentate nucleus of RLS patients (Astrakas et al., 2008). Furthermore, MRI demonstrated brain iron deficiency in the caudate head and thalamus medial/dorsal/ventral of idiopathic RLS patients (Godau et al., 2008). The authors suggested a multiregional (global) brain iron deficiency in RLS. Notably, this is the first neuroimaging study, where the RLS patients were unmedicated. At last, a recent study showed increased iron content in globus pallidus internal and subthalamic nucleus in unmedicated RLS patients, suggesting a dysfunction of the basal ganglia (Margariti et al., 2012).

In addition, a study determining brain iron status in the cerebrospinal fluid (CSF) exhibited decreased ferritin levels and increased transferrin levels in the CSF for RLS patients compared to healthy controls (Earley et al., 2000).On the other hand, there was no difference in serum ferritin and transferrin levels between the two groups. A further study, this time using insomnia patients as controls to exclude sleep loss as a confounding factor, reproduced these results. Furthermore, the CSF iron level was significantly lower in the RLS group of patients (Mizuno et al., 2005).

1.2.3 Anatomical regions implicated in RLS

In general almost every anatomical region involved in somatosensation and movement, such as motor and somatosensory cortex, striatum, thalamus, A11 region of hypothalamus, SN, inferior olive, red nucleus, cerebellum, spinal cord, anterior singulate nucleus and peripheral nervous system, has been implicated in the pathophysiology of RLS. Most of these regions are involved in the dopaminergic or opioid neurotransmission and have been reported by neuroimaging (MRI, PET, and ultrasound) or neuropathological studies.

MRI studies comparing changes in cerebral gray matter of RLS patients and more specifically in the somatosensory/motor cortex and thalamus, obtained contradictory results with a probable confounding factor being the medication of the patients. Studies with medication-naive patients did not reveal any significant alteration of the cerebral gray matter in RLS patients (Hornyak et al., 2007; Unrath et al., 2007; Celle et al., 2010). The studies implicating RLS pathophysiology in the striatum, thalamus, anterior cingulate gyrus and SN have been mentioned before as part of the dopamine and iron neuropathology.

The A11 dopaminergic neurons appeared normal in RLS autopsy brains, with normal TH (+) cell volume and no inflammation (Earley et al., 2009). Another study showed that iron deprivation and 6-hydroxydopamine (6-OHDA) lesions in A11 nuclei differentially altered the D1, D2, and D3 receptors' expression and binding capacity in the lumbar spinal cord of mice, which was accompanied by increase in locomotion (Qu et al., 2007; Zhao et al., 2007).

Regarding the spinal cord hypothesis, a study supported that PLMs in RLS and flexor reflex share common spinal mechanisms and suggested that PLMs may result from enhanced spinal cord excitability in RLS patients (Bara-Jimenez et al., 2000). Another study demonstrated diminished inhibition at spinal level in patients with PLMs. The authors assumed that this occured due to altered function of the descending spinal tracts, peripheral influence or changes at the inter-neural circuitry at the spinal level (Rijsman et al., 2005).

Functional MRI findings indicated that cerebellar and thalamic activation may occur during sensory leg discomfort and that the red nucleus and brainstem are involved in the generation of periodic limb movements in patients with RLS (Bucher et al., 1996).

Finally, a study examining the somatosensory processing in RLS patients revealed an impairment of temperature perception in 72% of the secondary RLS patients and in 55% of idiopathic RLS patients. The peripheral C-fibre function was normal in idiopathic RLS patients, supporting a dysfunction of central somatosensory processing, and abnormal in secondary RLS patients, supporting a small fibre neuropathy (Schattschneider et al., 2004).

1.2.4 Opioids

An alternative treatment for RLS as already mentioned is with opioids, especially in patients non-responsive to dopaminergics. The effects of opioids' treatment can be blocked by the opioid antagonist naloxone. This suggests a specific way of action, targeting the opioid receptor and implicates the endogenous opioid system (enkephalines and endorphines) in the pathophysiology of RLS (Walters et al., 1993; Winkelmann et al., 2001; Walters, 2002).

A PET scan study showed post-synaptic opiate receptor binding/availability in the pain system (thalamus, amygdala, caudate nucleus, anterior singulate gyrus, insula, and orbitofrontal cortex) that could compensate for the distressing RLS symptoms, which decreased in analogy with the severity of the RLS symptoms (von Spiczak et al., 2005).

A pilot post mortem study demonstrated 30% decrease of the endogenous opioids beta endorphin and metenkephalin in the thalamus of RLS patients in comparison with controls (Walters et al., 2009). The same group showed that the δ-opioid peptide [*D*-Ala2, *D*-Leu5]Enkephalin (DADLE) protected the SN dopaminergic cells of rats from induced apoptosis by iron deficiency (Sun et al., 2011). This suggests once more that opioid treatment may protect the dopamine system from dysfunction.

1.2.5 Genetics

The first time that RLS was described as a hereditary disorder was from Oppenheim in 1923 (Oppenheim, 1923). In 1960 Ekbom described that one-third of his patients appeared with a familiar form of the disease (Ekbom, 1960). Several studies showed that 50-60% of the patients present a positive family history, especially the patients with idiopathic RLS (Walters et al., 1996; Montplaisir et al., 1997; Winkelmann et al., 2000; Allen et al., 2002; Winkelmann et al., 2002).

The RLS prevalence is higher among first- and second-degree relatives of individuals with RLS than among relatives of individuals without RLS (Allen et al., 2002). To identify the genetics underlying the RLS pathophysiology epidemiological genetic studies were employed, such as linkage and genome wide association studies (GWAS) along with studies of twins and strongly affected families. These analyses revealed the complex nature of RLS genetics.

1.2.5.1 Twin studies and family studies

Studies on monozygotic and dizygotic twins can reveal the contribution of genetic and environmental determinants to a trait. Research carried out on twins demonstrated a higher concordance rate for the monozygotic in comparison with the dizygotic twins, a fact that accounts for genetic influence (Ondo et al., 2000).

Another study on twins, which holds a possible recruitment bias (advertisement calling for identical twins with RLS), estimated the heritability to be 0.6 (Desai et al., 2004). This pointed to genetic and non-genetic effects contributing to the risk for RLS.

A segregation analysis is used to determine the mode of inheritance of a phenotype from family data, in order to identify major gene effects and disease causing genes. Segregation analysis was applied for 238 families (only first degree relatives included) and suggested a bimodally distributed mode of inheritance dependent on the age of RLS onset (Winkelmann et al., 2002). The involvement of a major gene was implicated with an autosomal dominant fashion of inheritance and an additional multifactorial component, in families with an earlier age at onset. In families with late age at onset an inheritance model of free transmission probabilities was implied, but a co-dominant or a recessive model could not be excluded. This study refers to the possibility that RLS is a genetically heterogeneous disease.

Another segregation analysis performed on 77 pedigrees identified a single-locus Mendelian dominant model with gender as a covariate, with an allele frequency of 0.077 and complete penetrance (Mathias et al., 2005). All non-genetic models were rejected.

Linkage studies are also family based and aim to identify rare genetic variants with strong effects that are segregating within a family parallel and consistently with the

disease of interest. They are based on the observation that short haplotypes tend to be passed on to the next generation intact, without any recombination event.

In this way linkage studies have identified up to date several RLS loci (RLS1-5) in various chromosomes (chr.12, chr.14, chr.9, chr.20, chr.19). No causal gene has been though identified. The RLS1 locus was identified with the logarithm of the odds score analysis based on the assumption that RLS follows a recessive mode of inheritance in the examined family (Desautels et al., 2001; Desautels et al., 2005; Winkelmann et al., 2006). All the remaining loci were identified based on an autosomal-dominant model of inheritance (Bonati et al., 2003; Chen et al., 2004; Levchenko et al., 2004; Levchenko et al., 2006; Liebetanz et al., 2006; Pichler et al., 2006; Kemlink et al., 2007; Kemlink et al., 2008; Lohmann-Hedrich et al., 2008).

Generally, all these studies only estimate a model of inheritance and most of the time deal with highly heterogeneous samples, which has to be considered. The several genetic loci linked to RLS, as well as the high intrafamilial heterogeneity corroborate once more the notion that RLS is a genetically heterogeneous complex trait, determined by various genetic and environmental factors.

Nowadays, rare causal variants can be identified by high throughput next generation sequencing technology. A recent study used this technology to sequence the exome of a family with autosomal dominantly inherited RLS (Weissbach et al., 2012). It identified rare variants (missense and splice) in four genes and suggested one of them, the protocadherin-alpha 3 (*PCDHA3*) as a plausible candidate gene for RLS. The missense variant segregated in the family and did not appear in 250 controls. This gene is expressed in neurons and mediates neuronal interaction (Wu et al., 2000). It also plays

an important role in the neuronal development (El-Amraoui et al., 2010). In conclusion, these findings need to be interpreted with caution, as the coverage of exome sequencing was incomplete, phenocopies may have been included and the non-coding part of the genome was not sequenced. Additionally, the study was not replicated and represents only a single observation. Thus, the true-disease causing mutations may have been missed.

1.2.5.2 Genome wide association studies

Genome wide association studies aim to identify single nucleotide polymorphisms (SNPs) that present with a higher frequency in the affected group compared with the control group (which most of the times is population based) and increase the risk to acquire the associated phenotype.

Genetic variants within six genes have been associated with RLS. The first genome wide association study for RLS identified genetic variants increasing the risk for RLS in Meis homeobox 1 (*MEIS1*) (2p, intronic locus), in bric-à-brac, tramtrack and broad (BTB)/ pox virus and zinc finger domain containing 9 (*BTBD9*) (6p, intronic locus) and the intergenic region of SKI family transcriptional corepressor 1 - mitogen-activated protein kinase kinase 5 (*SKOR1-MAP2K5*) (15q) genes (Winkelmann et al., 2007). The results of the exploratory study were confirmed by two independent replication studies in different populations. The variants identified were common variants with minor allele frequency (MAF) greater than 10% and low effect size. After fine mapping, haplotype analysis for *MEIS1* delineated a haplotype block (rs6710341 and rs12469063) more strongly associated with RLS than each single SNP in the block. These three loci account for a large part (more than 50%) of the phenotype in the populations studied.

This is the first study that identifies genes implicated in development and suggests a possible developmental origin of RLS.

In an independent study a common intronic variant in *BTBD9* was associated with PLMS and not with RLS in two Icelandic and an American population (Stefansson et al., 2007).

A further study identified association of RLS with the protein tyrosine phosphatase, receptor type D (*PTPRD*) gene, adding a fourth genome-wide significant locus for RLS again in a gene that has a developmental component (Schormair et al., 2008). The association signal is located in the 5' untranslated region (5' UTR) of *PTPRD* at 9p23-24, known also from the linkage studies as RLS3 locus. Further analysis revealed no mutations in the exons of *PTPRD* and no exon deletions or duplications among nine affected individuals of an RLS3-linked family. Thus, no rare alleles with strong effects that could explain the linkage signal were identified. In addition, the familial relative risk was too low, rendering this signal unable to explain the original RLS3 linkage signal and probably independent. The associated SNPs are common with MAF greater than 13% and show weak effects with odds ratio less than 1.5.

Finally, a recent genome wide association study replicated once more the association of the four known loci (*MEIS1*, *BTBD9*, *PTPRD* and *SKOR1-MAP2K5*) and identified two novel ones in a population of European ancestry (Winkelmann et al., 2011). The novel RLS-associated common variants reside in an intergenic region 1.3 Mb downstream of *MEIS1* (2p14) and in 5' UTR of TOX high mobility group box family member 3 (*TOX3*) gene and the adjacent non-coding RNA BC034767 (16q12.1).

In conclusion, genome wide association studies identified common variants with small effect sizes for RLS in six genomic loci **(Figure 1.1, Table 1.1)**. Intriguingly, most of the

genes associated are developmental and involved in the spatiotemporal cell specification. There is no obvious link of the associated genes with iron or dopamine metabolism, but this does not exclude a relationship of these genes with iron or dopamine homeostasis. These findings opened a new chapter in the pathophysiology of RLS implicating a developmental component.

Figure 1.1 depicts the Manhattan plot of the third GWAS, illustrating the six loci rendering genetic variants that increase the risk for RLS. This study included almost one thousand cases for the association and 3,935 cases for the replication, which makes it the largest association study for RLS at the moment (Winkelmann et al., 2011). **Table 1.1** shows the association results of this GWA, the joint analysis and replication.

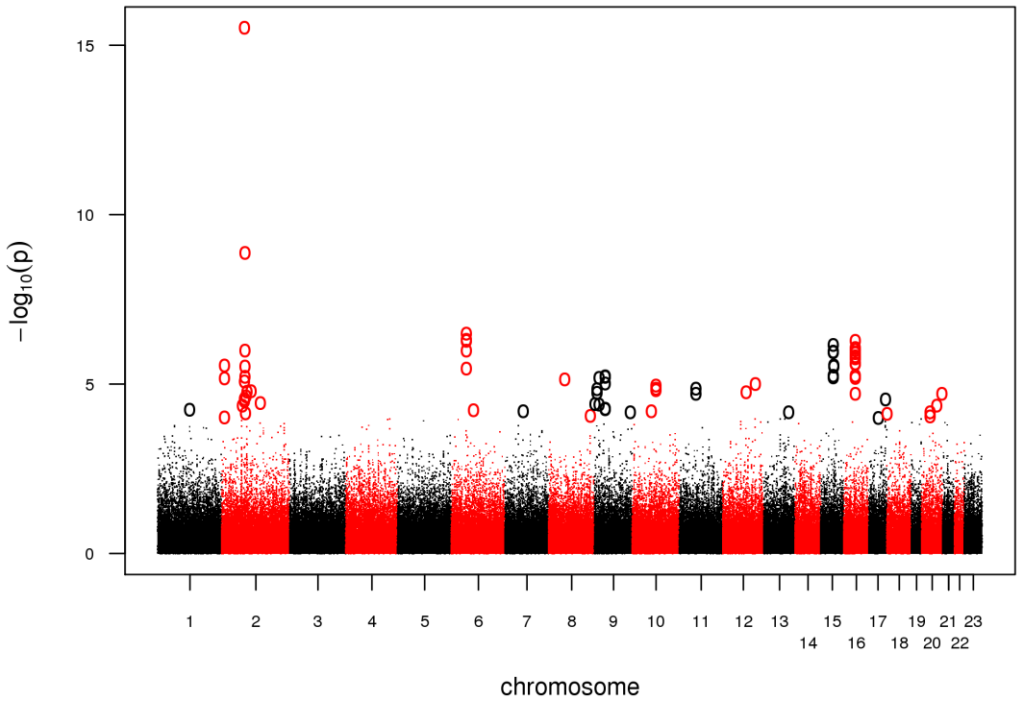

Figure 1.1. Manhattan plot of the GWA *(from Winkelmann et al., 2011)*

Association results of the GWA stage. The x-axis represents genomic position along the 22 autosomes and the x-chromosome, the y-axis shows $-\log_{10}(P)$ for each SNP assayed. P stands for significance. SNPs with a nominal λ-corrected $P<10^{-4}$ are highlighted as circles.

Chr	Locus	LD block (Mb)	SNP	Position (bp)	Risk allele	Risk allele frequency cases/controls	P_{GWA}	$P_{REPLICATION}$	P_{JOINT}	Odds ratio (95% CI)
Known risk loci (1 SNP per locus)										
2	MEIS1	66.57-66.64	rs2300478	66634957	G	0.35 / 0.24	7.77×10^{-16}	4.39×10^{-35}	3.40×10^{-49}	1.68 (1.57-1.81)
6	BTBD9	37.82-38.79	rs9357271	38473851	T	0.82 / 0.76	6.74×10^{-7}	2.01×10^{-16}	7.75×10^{-22}	1.47 (1.35-1.47)
9	PTPRD	8.80-8.88	rs1975197	8836955	A	0.19 / 0.16	4.94×10^{-5}	1.07×10^{-6}	3.49×10^{-10}	1.29 (1.19-1.40)
15	MAP2K5/ SKOR1	65.25-65.94	rs12593813	65823906	G	0.75 / 0.68	1.49×10^{-6}	1.54×10^{-17}	1.37×10^{-22}	1.41 (1.32-1.52)
New genome-wide significant loci ($P_{JOINT} < 5.2 \times 10^{-8}$)										
2	intergenic region	67.88-68.00	rs6747972	67923729	A	0.47 / 0.44	1.37×10^{-6}	3.73×10^{-6}	9.03×10^{-11}	1.23 (1.16-1.31)
			rs2116050	67926267	G	0.49 / 0.47	7.84×10^{-6}	4.85×10^{-6}	4.83×10^{-10}	1.22 (1.15-1.30)
16	TOX3/ BC034767	51.07-51.21	rs3104767	51182239	G	0.65 / 0.58	7.38×10^{-7}	2.16×10^{-13}	9.40×10^{-19}	1.35 (1.27-1.43)
			rs3104788	51196004	T	0.65 / 0.58	1.19×10^{-6}	2.42×10^{-13}	1.63×10^{-18}	1.33 (1.25-1.43)

Table 1.1. Association results of GWA and joint analysis of GWA and replication
(from Winkelmann et al., 2011)
This table depicts the RLS-associated SNPs with genome-wide significance. P_{GWA} stands for the λ-corrected nominal P-value of GWA stage, $P_{REPLICATION}$ for nominal P-value obtained from meta-analysis of the replication stage samples and P_{JOINT} for nominal P-value of the joint meta-analysis of GWA and replication stage, λ -corrected in samples, where λ-values were available. Nominal P-values in GWA were calculated with logistic regression. For nominal $P_{REPLICATION}$ and P_{JOINT} -values a fixed-effects inverse-variance meta-analysis was performed. Risk allele frequencies and OD were calculated in the joint sample. LD blocks were defined by D' using Haploview 4.2 based on HapMap CEU population data from HapMap release #27. CI stands for 95% confidence interval and LD for linkage disequilibrium. Genome positions refer to the Human March 2006 (hg18) assembly.

The role of the genetic risk factors identified by GWA studies for idiopathic RLS was investigated in patients with end stage renal disease (ESRD) and RLS (Schormair et al.,

2011). We found that variants in *MEIS1* and *BTBD9* were associated with RLS in ESRD and a trend for association to *MAP2K5/SKOR1* and *BTBD9* in the Greek sample, whose size was smaller. In a combined analysis for both samples *BTBD9* was the only associated gene. This was the first demonstration of a genetic influence on RLS in ESRD patients.

Up to date, there is no recognized single mutation causing RLS. To conclude, the existence of many genetic loci that contribute only weakly to the disease implicates a multifactorial pathophysiology with a combination of genetic and environmental factors.

1.3 Restless legs syndrome, MEIS1 and other associated genes

Variants within the *MEIS1* gene demonstrated the strongest association with RLS. However, the functional relevance of *MEIS1* genetic association with RLS remains unraveled. *MEIS1* is a member of a family of highly conserved three amino acid loop extension homeobox genes. This gene includes eleven exons and occurs with 18 splice variants (Ensembl, genome assembly: GRCh37).The protein coded by *MEIS1* is expressed in many regions of the developmental mouse and adult human brain, such as forebrain, midbrain (basal ganglia) and hindbrain (Allen Brain Atlas, http://www.brain-map.org).

MEIS1 encodes a homeodomain transcription factor involved in multiple developmental processes in vertebrates. In general, the homeobox gene *MEIS1* plays a critical role in the development of mouse, chicken, axolotl and Drosophila limbs (Mercader et al., 1999; Mercader et al., 2005). The restriction of this protein to proximal regions of the limb is essential to specify cell fates and differentiation patterns along the proximodistal axis of

the limb, with retinoic acid and fibroblast growth factor as its upstream regulators (Mercader et al., 2000).

The Xenopus homolog for *MEIS1* is involved in neural crest cell fate specification during embryogenesis (Maeda et al., 2001). In developing Xenopus embryos Meis1 showed a broad expression pattern with strong expression in tissue of neural fate, such as midbrain, hindbrain, neural tube and neural crest derived branchial arches. Overexpression or misexpression of an alternative spliced form of Meis1 induced expression (ectopically in the case of misexpression) of neural crest markers.

Furthermore, the lateral precursors in the developing olfactory epithelium of mouse express high levels of Meis1 and induce multi-potent self-renewing and slowly dividing neural stem cells (Tucker et al., 2010). In this case Meis1 along with Sox2 regulate the transmission from lateral to medial precursor state. The latter gives rise to transit amplifying neurogenic progenitors of olfactory receptor, vomeronasal and gonadotrophin releasing hormone neurons.

In the zebrafish visual system Meis1 is regulating Bmp signaling and specifies temporal identity in the retina as well as pattering of the tectum (Erickson et al., 2010). In this way Meis1 establishes the retinotectal map and organizes the zebrafish visual system.

Meis1 is essential for hematopoiesis and vascular pattering in the mouse embryo (Azcoitia et al., 2005). Inactivation of Meis1 in mice resulted in embryonic death from embryonic days (E) E11.5 to E14.5. The embryos presented hemorrhage, liver hypoplasia, anemia, underdevelopment of the hematopoietic stem cell compartment and complete agenesis of the megakaryocyte lineage.

The stability of DNA binding by heterotrimers of MEIS1, PBX and HOX proteins is enhanced relative to the heterodimers of either MEIS1/HOX and PBX/HOX alone (Shanmugam et al., 1999). Hox transcriptional network specifies the spinal motor neuron pool identity and target-muscle connectivity, acting as transcriptional partner of Meis1 (Dasen et al., 2005). By excluding or ectopically expressing Meis1 in different motor neuron columns this study showed that Meis1 is essential for pattering of many motor neuron pools in the spinal cord of chick embryos. The specificity of this regulatory network and its connections is critical to locomotor behavior. Intriguingly, spinal hyperexcitability is a component in the development of PLMS, a common feature of RLS patients (Bara-Jimenez et al., 2000). Furthermore, Meis1 together with Hoxa9 proteins are known to be strong oncogenic factors in the induction of acute myeloid leukemia (Thorsteinsdottir et al., 2001).

A Canadian study demonstrated reduced expression of *MEIS1* (decreased mRNA and protein levels) in lymphoblastoid cell lines and brain tissue (thalamus) from RLS patients, possibly through intronic *cis*-regulatory elements. The patients were homozygous for an intronic RLS risk haplotype (Xiong et al., 2009).

The strongest RLS-associated signal from GWAS expands 32 kb in intron eight, exon and intron nine of *MEIS1* and defines a strong Linkage Disequilibrium (LD) block (**Figure 1.2**) (Winkelmann et al., 2007). The strongest signal was the highly correlated pair of SNPs (LD r^2 =0.97; rs12469063 $P_{nom}= 7.7\times10^{-18}$ and rs2300478 $P_{nom}= 4.2\times10^{-18}$). A conditional analysis with rs12469063 as covariate identified a risk haplotype with rs6710341 ($P_{nom}= 5.2\times10^{-12}$), which raised the RLS risk from an OR of 1.7 to 2.8 (frequency=0.168).

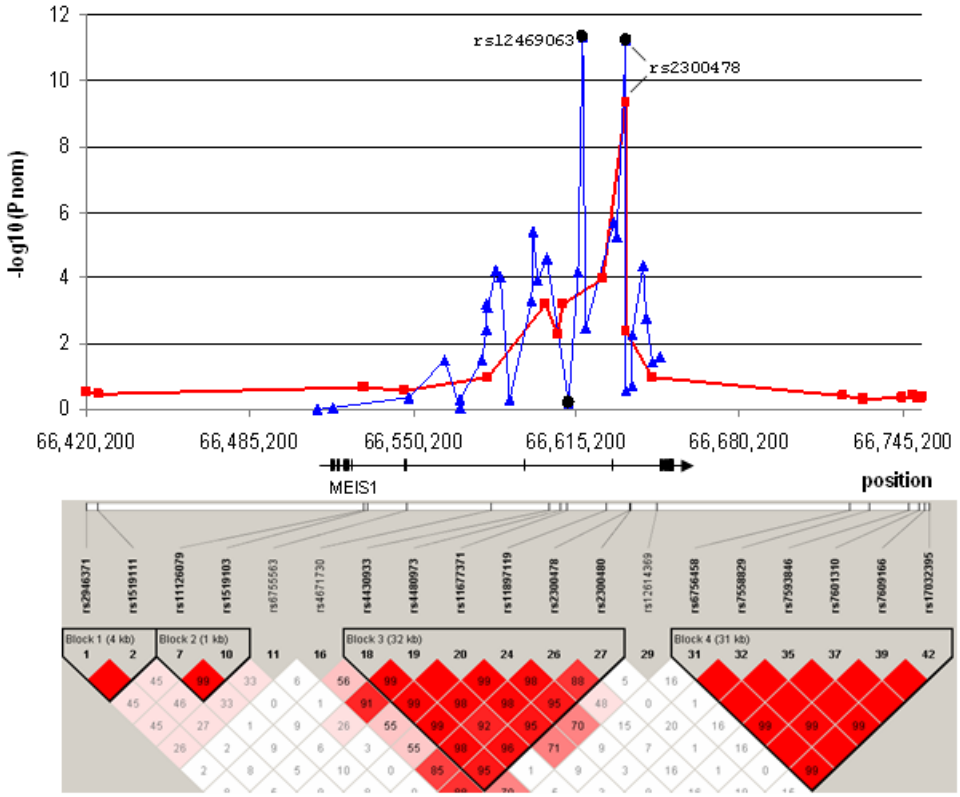

Figure 1.2. Pairwise LD diagram for *MEIS1*-associated locus *(from Winkelmann et al., 2007)*

The P values based on the stage 1 Affymetrix data clearly delineate the regions of interest within a single LD block in the limits of the transcribed genomic unit for *MEIS1*. Pairwise LD, measured as D', was calculated from the stage 1 control data set using the methods of Gabriel as implemented in Haploview. Shading represents the magnitude and significance of pairwise LD, with a white to- red gradient reflecting lower to higher LD values. Stage 1 Affymetrix SNPs are indicated by red squares, replication SNPs (Stage 2a) by black circles and fine mapping SNPs (Stage 2b) by blue triangles. X-axis shows genomic position, and y-axis shows -$\log_{10}$(P). Transcriptional units are indicated by black arrows, with exons depicted as black bars.

Another gene identified by GWAS for RLS is *BTBD9*. *BTBD9* encompasses eleven exons and has eight transcripts. It codes for a protein that belongs to the BTB complex transcription regulators (Numoto et al., 1993; Bardwell et al., 1994). BTB is a protein-protein interaction motif that demonstrates plenty of functions, such as ion channel

gating (Kreusch et al., 1998), cytoskeleton dynamics (Ziegelbauer et al., 2001), and protein ubiquitination for degradation (Wilkins et al., 2004). In Drosophila the bric-à-brac (bab) gene, which contains also the BTB domain as *BTBD9*, is required for pattern formation along the proximal-distal axis of the leg and antenna (Godt et al., 1993). Variants in *BTBD9* are also associated with Tourette syndrome, which is characterized by hyperkinesias (Riviere et al., 2009).

MAP2K5 has also been associated with RLS, includes 22 exons and has twelve transcripts. MAPK pathway is activated by diverse extracellular and intracellular stimuli and is involved in several cellular processes, including cell proliferation, differentiation, survival and death (Torii et al., 2006; Dhillon et al., 2007). Dysregulation of this pathway has been implicated in a variety of neurological diseases, such as Alzheimer's disease (Marques et al., 2003), Parkinson's disease (Silva et al., 2005), amyotrophic lateral sclerosis (Bendotti et al., 2005), as well as in cancer (Lochhead et al., 2012). The MAP2K5/ERK5 cascade is important for early stages of muscle differentiation and neuroprotection of dopaminergic neurons (Dinev et al., 2001; Cavanaugh et al., 2006).

SKOR1 includes fifteen exons and has five splice variants. This gene codes for a homeobox protein that acts as transcriptional repressor of Lbx1 (Mizuhara et al., 2005). Lbx1 plays a critical role in the development of sensory pathways in the dorsal horn of spinal cord that relay pain and touch (Gross et al., 2002). In addition, Lbx1 is important for the specification of dorsal interneurons and might act together with Pax3 to promote neural tube closure (Kruger et al., 2002).

The RLS-associated gene *PTPRD* incorporates 45 exons and has ten transcripts. PTPR-sigma and PTPR-delta are complementary to each other during mammalian

development and are responsible for proper motor neuron axon targeting during mammalian axonogenesis (Uetani et al., 2006). The 5' UTR region of this gene consists of eleven noncoding exons and is found to be aberrantly spliced or with microdeletions in neuroblastoma primary tumors and cell lines (Nair et al., 2008). The researchers of this study concluded that the 5’ UTR of this gene is essential in stabilizing its mRNA.

Finally, *TOX3* is the most recent RLS-associated gene, includes seven exons and has five transcripts. *TOX3* has been associated with breast cancer in many GWAS (Easton et al., 2007). It is known that it interacts with CREB and is involved in mediating calcium-dependent transcription in neurons (Yuan et al., 2009).

It is not known whether RLS has a developmental component and the associated genetic factors predispose to the disease in development or play a role only in adulthood. It also remains unclear which anatomical region is involved in the pathophysiology of RLS. Unraveling the pathophysiology of RLS in its genetic context will provide insight into the regulatory networks of developmental genes, such as *MEIS1*. This will in general enlighten the scientific community about sensorimotor interactions and disorders. The *MEIS1* homeobox gene is one of the most conserved genes through evolution and comprises an intronic association signal for RLS. Since no changes in exon and splice site sequences of *MEIS1* could be found in RLS patients, the study of genomic conservation might give us a better understanding of the function and importance of non-coding regions, which are conserved through different species.

1.4 Aim and research objectives of my doctoral work

During my doctoral work, my aim was to examine the functional role of the RLS-associated intronic non-coding region of *MEIS1*, using dual luciferase assays and identify the regions that are putative regulatory elements. Furthermore, by comparing the expression of the protective with the risk allele, I investigated the functional effect of RLS variants associated with the disease phenotype. Overall, my research goal was to reveal the regulatory network of MEIS1 in RLS, by unraveling the upstream and downstream factors of *Meis1* that are relevant for the disease.

2 RESULTS

2.1 High conservation of the RLS-associated *MEIS1* locus

High level of DNA conservation often indicates biologically important function, such as regulation of gene expression, in other words an activity of an enhancer or a silencer (Allende et al., 2006). We compared the RLS-associated *MEIS1* locus (32 kb LD block) of human with several *MEIS1* orthologs (mouse, chicken, frog, pufferfish) using vista and UCSC browser, and identified seven highly conserved non-coding regions (HCNRs) **(Figure 2.1, Figure 2.2)** (Dubchak et al., 2000; Rosenbloom et al., 2012). Six HCNRs (HCNRs 602, 612, 617, 622, 629, 631) accommodate SNPs associated with RLS and one of them (HCNR 606) doesn't carry any variants associated with RLS. In both figures the 32 kb LD block is depicted, which occupies part of intron eight, exon nine and part of intron nine of MEIS1 gene. In **Figure 2.2** data from the ENCODE project has been included, such as DNase clusters and chromatin immunoprecipitation (ChIP) data from transcription factor binding (Rosenbloom et al., 2012). The ENCODE project (Encyclopedia of DNA Elements) aims to characterize all functional elements in the human genome. DNase clusters display DNase hypersensitive areas assayed in a large collection of cell types. Regulatory regions tend to be DNase sensitive. The Txn Factor ChIP track shows regions, where transcription factors, proteins responsible for modulating gene transcription, bind to DNA as assayed by ChIP-seq (with antibodies specific to the transcription factor followed by sequencing of the precipitated DNA). The RLS-associated *MEIS1* locus appears in an open chromatin mode, in the DNA cluster track, and binds various transcription factors, in the ChIP track. Thus, both of these

ENCODE tracks further support our hypothesis that the RLS-associated *MEIS1* locus encompasses regulatory function.

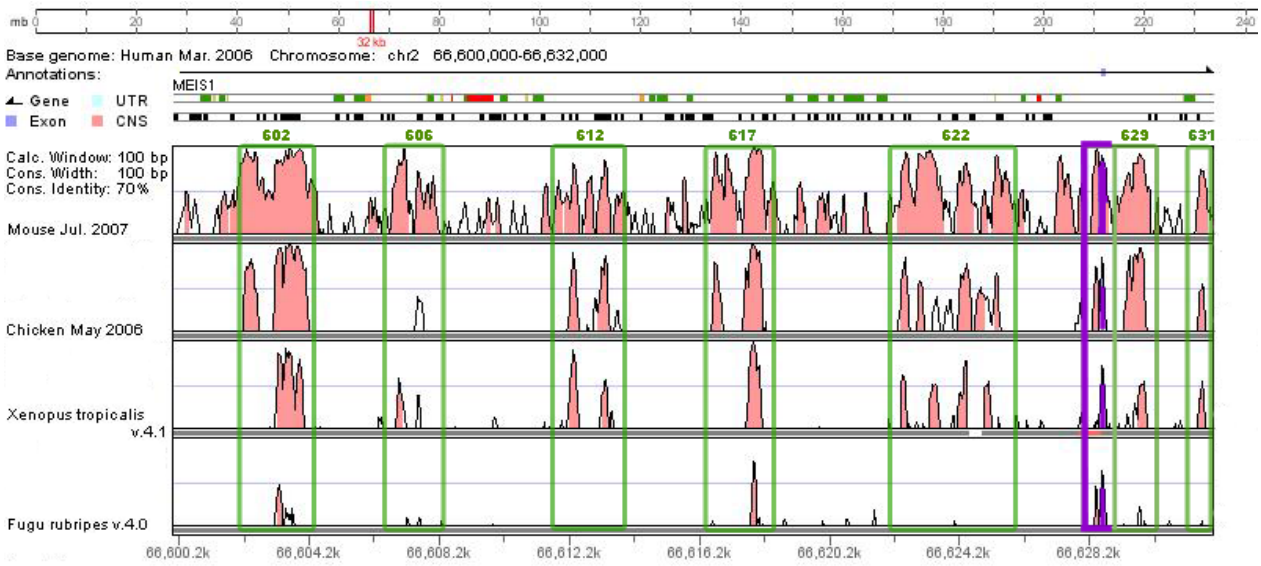

Figure 2.1. Conservation of the human RLS-associated *MEIS1* locus
(generated in Vista Browser, http://pipeline.lbl.gov/cgi-bin/gateway2)
The graph demonstrates the alignment of the human 32 kb LD block (Mar.2006) with the mouse (Jul. 2007), chicken (May 2006), frog (Xenopus tropicalis v.4.1) and pufferfish (Fugu rubripes v.4.0) homolog sequence. The exon nine of MEIS1 gene is depicted with lilac color. Red and delineated with green color are the seven highly conserved non-coding regions (HCNRs 602, 606, 612, 617, 622, 629, and 631) that have been selected for further analysis.

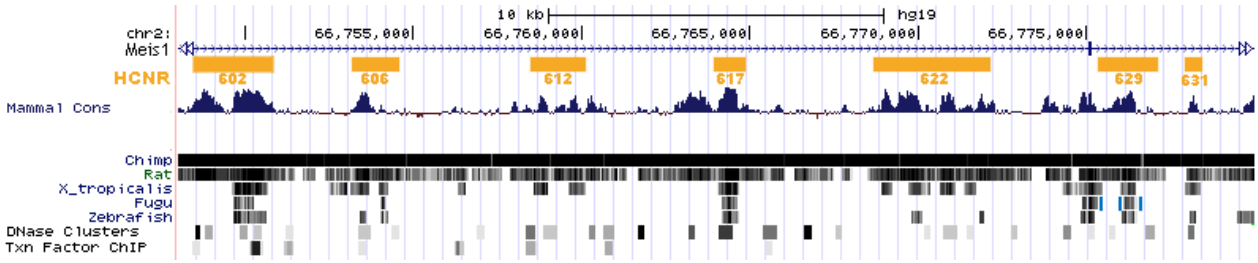

Figure 2.2. Conservation and regulatory information of the human RLS-associated *MEIS1* locus

(generated in UCSC Genome Browser, http://genome.ucsc.edu/)

In orange color the seven HCNRs are depicted on the genome. Below follows the conservation of these regions in mammals, chimpanzee, rat, frog, pufferfish, and zebrafish. The last two tracks are based on ENCODE data and demonstrate that most of the HCNRs present an open chromatin form and bind transcription factors, something that implies regulatory potential.

2.2 Functional highly conserved non-coding regions associated with RLS

After the delineation of the putative regulatory elements through their conservation, I moved to a functional reporter assay, the dual luciferase assay. I used this assay to examine the functionality of all seven HCNRs, in other words to examine, if they exhibit a putative enhancer or silencer activity in different cell lines.

Indeed, all seven HCNRs showed regulatory function in the 293T cell line with different effect sizes depending on the construct, as shown in **Table 2.1.** Three HCNRs, 606, 629 and 631, presented as enhancers, with almost two (small effect size), ten and four fold of increase in the relative luciferase expression respectively **(Figure 2.3)**. The 631 HCNR showed a SNP dependent differential expression, with the risk allele showing 1.33 fold decreased relative luciferase expression. The HCNR 606 showed also differential expression between the two alleles (A versus C allele). However, this SNP

was not further examined, since it is not associated with RLS. It is possible though that this SNP plays a functional role in another phenotype than RLS.

HCNR	602	606	612	617	622	629	631
Size (bp)	2375	1425	1601	944	3507	1766	480
Function in reporter assay (DLA)	Silencer Small effect (1.28)	Enhancer Small effect (1.90)	Silencer Big effect (3.13)	Silencer Big effect (3.70)	Silencer Small effect (1.25)	Enhancer Big effect (10.42)	Enhancer Big effect (4.00)
Significant allele-specific effect	No	Yes	No	No	Yes	No	Yes

Table 2.1. Overview of the HCNRs examined with dual luciferase assays
All examined HCNRs are listed together with their size (length in base pairs-bp) and their function in dual luciferase assays in the 293T cell line. The number in parenthesis states the fold difference of the relative luciferase units (RLU) compared with the control vector. The last row specifies the presence of a statistically significant allele-specific difference in luciferase expression.

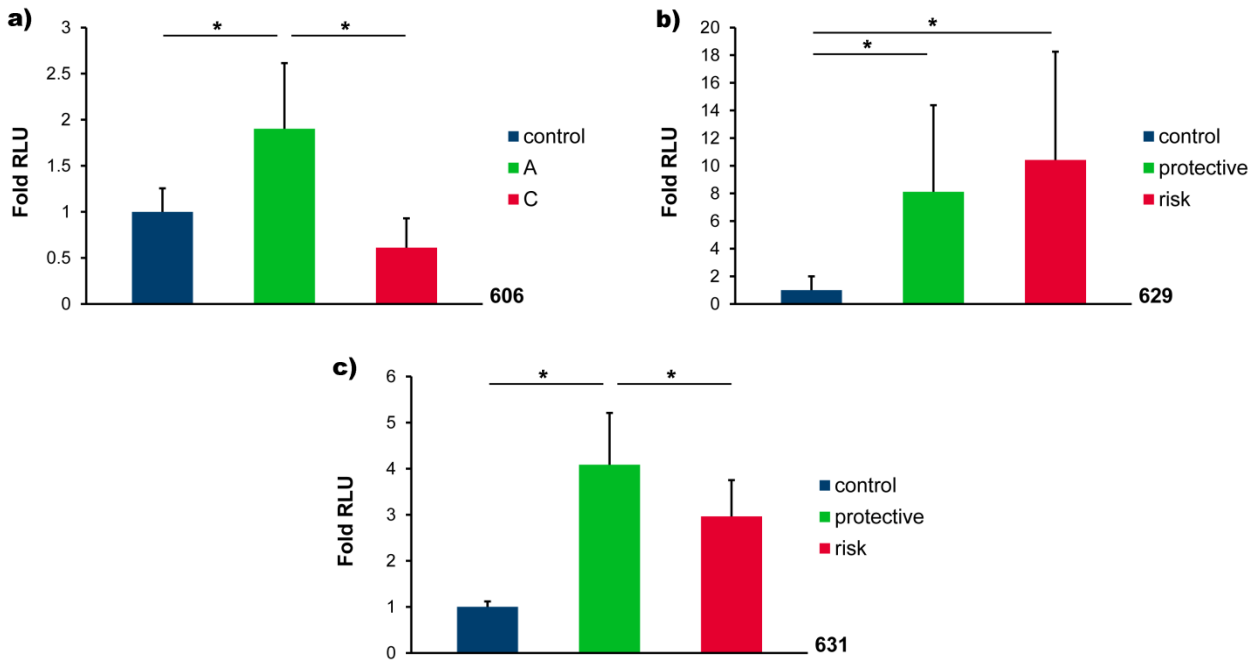

Figure 2.3. The HCNRs 606, 629 and 631 function as enhancers in 293T cell line
The 293T cell line was transfected with the vector carrying the HCNR construct with either the protective alleles (green color) or the risk alleles (red color). All three constructs (HCNRs 606, 629, 631) functioned as enhancers, by enhancing luciferase expression 1.9-fold, 10.42-fold, and 3.7-fold respectively. The risk alleles of HCNRs 606 and 631 decreased the enhancer activity for 3.11-fold and 1.33-fold, respectively. The empty vector without any insert was used as the control vector (blue color) and its activity was set to 1. Data represent the means and standard deviations of at least six technical replicates in each of the three experimental replicates. They demonstrate the fold change of the RLU compared to the empty vector. Asterisks indicate statistically significant differences, with *p< 0.016 (Wilcoxon rank sum test, value corrected for multiple testing).

In addition, four HCNRs, 602, 612, 617 and 622 presented as silencers. HCNRs 602 and 622 reduced the reporter gene's expression in a weak manner with less than two-fold decrease of RLU. In the case of HCNR 622 only the protective allele functioned as a silencer with a weak effect (1.25 fold). However, the vector carrying the risk allele of HCNR 622 behaved as the control empty vector. For this reason, the SNP within

HCNR 622 was not further examined. However, HCNRs 612 and 617 showed a stronger effect with threefold and fourfold decrease of the relative luciferase expression, respectively **(Figure 2.4)**.

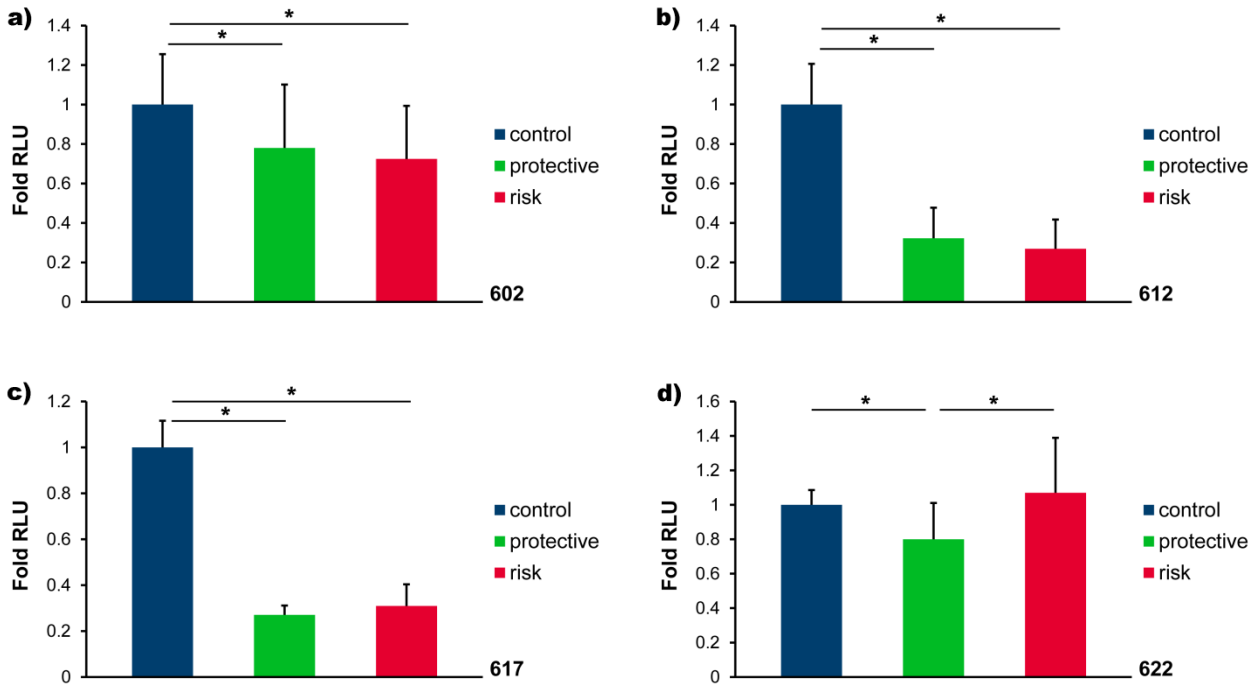

Figure 2.4. The HCNRs 602, 612, 617 and 622 function as silencers in 293T cell line
The 293T cell line was transfected with the vector carrying the HCNR construct with either the protective alleles (green color) or the risk alleles (red color). All four constructs (HCNRs 602, 612, 617, 622) functioned as silencers, by reducing luciferase expression 1.28-fold, 3.13-fold, 3.7-fold and 1.25-fold, respectively. The empty vector without any insert was used as the control vector (blue color) and its activity was set to 1. Data represent the means and standard deviations of at least six technical replicates in each of the three experimental replicates. They demonstrate the fold change of the RLU compared to the empty vector. Asterisks indicate statistically significant differences, with *p< 0.016 (Wilcoxon rank sum test, value corrected for multiple testing).

These results reveal a putative functionality hidden behind the *MEIS1* association signal for RLS. The genome-wide association studies indicated a region that incorporates *cis*-

regulatory elements. These *cis*-regulatory elements function as enhancers or silencers and regulate gene expression.

I should mention here that colleagues used a similar approach in parallel to examine the functionality of these elements with a reporter assay and green fluorescent protein (GFP) as the reporter gene in the zebrafish animal model (Knauf F. in collaboration with Casares F, Gómez-Skarmeta JL, Centro Andaluz de Biología del Desarrollo, Consejo Superior de Investigaciones Cientificas/ Universidad Pablo de Olavide, Seville, Spain). Of all HCNRs assayed, solely HCNR 617 exhibited both a reproducible neural expression pattern and a genotype-specific expression comparing the protective- and risk-allele reporter constructs. Zebrafish embryos carrying the risk allele showed an almost abolished enhancer function. The results of this screen are discussed in more detail in the discussion part.

Based on the results of the reporter assays, I focused on HCNR 617 and HCNR 631 and continued with further experiments, as both functioned as enhancers and showed allele-differential expression in the zebrafish animal model and in the 293T cell line, respectively.

2.3 A *cis*-regulatory element residing in the strongest RLS-associated region

The HCNR 617 carries the lead SNP rs123469063 that showed the strongest association signal for RLS (P_{nom}=7.7x10^{-18}). It also demonstrated an enhancer function for the protective allele, with a dramatic reduction of the enhancer's signal in the case of the risk allele, in the zebrafish animal model. Therefore, I have selected the HCNR 617 for further investigation with dual luciferase assays in different cell lines, such as

HEK293, HeLa, COS-7 and two neuroblastoma cell lines, SHSY-5Y and IMR32. All cell lines showed the same effect as a silencer, by suppressing luciferase expression, ranging from three to almost six fold difference **(Figure 2.5)**. In SHSY-5Y cells, I observed a small (0.73 fold), but statistically significant difference between the protective and risk allele. In this case the risk allele reduces the suppression of the reporter gene's expression. The only cell line that showed an allele-specific difference in the luciferase expression is a neuroblastoma cell line (SHSY-5Y). This cell line might resemble more the mammalian nervous system environment and its regulatory repertoire might include factors that are expressed also in the nervous system. It is possible that the transcription factors responsible for the enhancer activity in zebrafish are silenced or missing in all remaining cell lines.

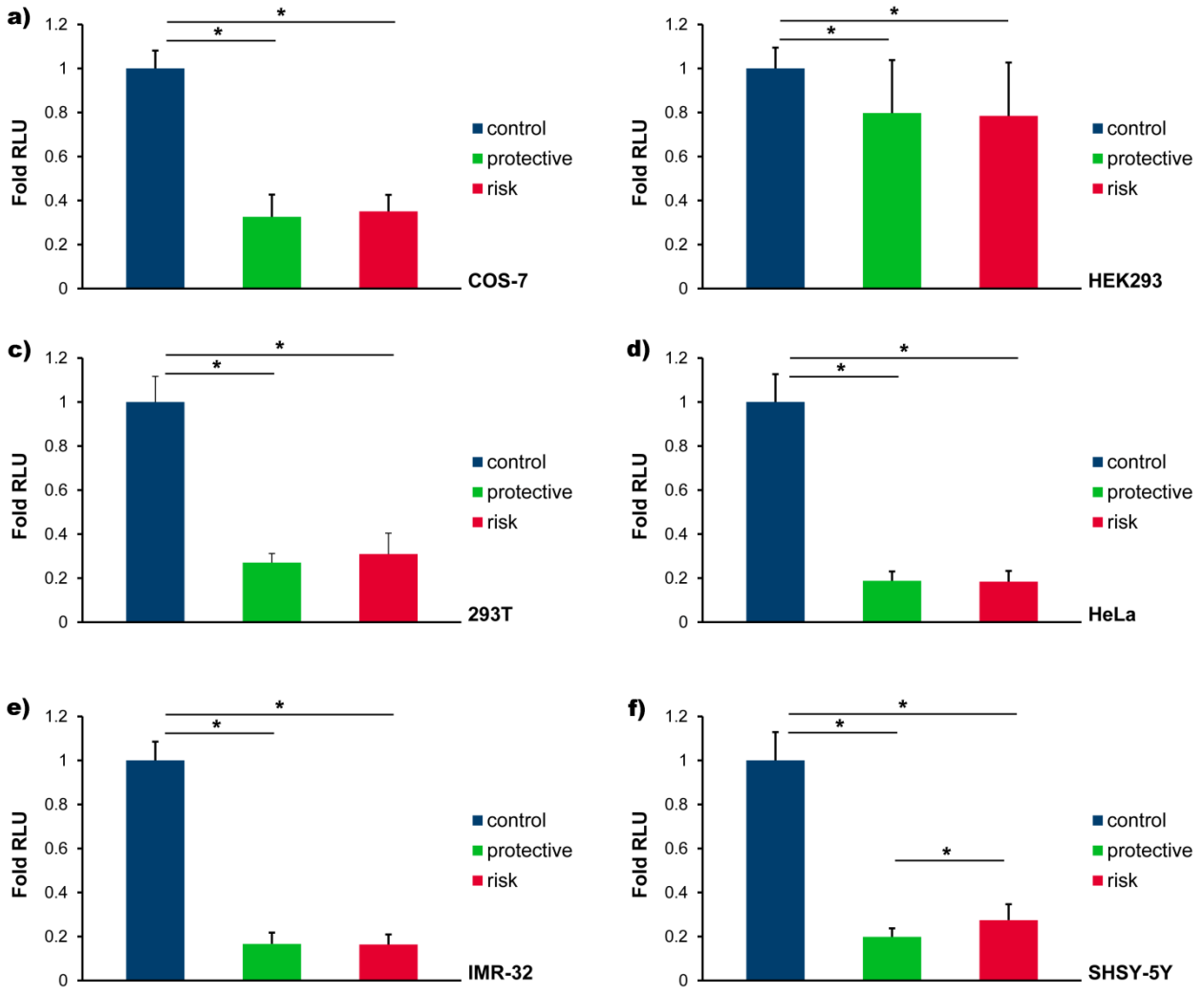

Figure 2.5. The HCNR 617 functions as a silencer in various cell lines

Several cell lines such as COS-7, HEK293, 293T, HeLa, IMR-32 and SHSY-5Y, were transfected with the vector carrying the 617 construct either with the protective alleles (green color) or the risk alleles (red color). In all cell lines both constructs functioned as silencers, by suppressing luciferase expression, ranging from 1.25- to 5.88-fold difference. In SHSY-5Y cells, I observed a small (0.73 fold), but statistically significant difference between the protective and risk allele, with the risk allele showing a higher expression than the protective one. The empty vector without any insert was used as the control vector (blue color) and its activity was set to 1. Data represent the means and standard deviations of at least six technical replicates in each of the three experimental replicates. They demonstrate the fold change of the RLU compared to the empty vector. Asterisks indicate statistically significant differences, with *p< 0.016 (Wilcoxon rank sum test, value corrected for multiple testing).

Here it is important to mention that after the screening in zebrafish and cell lines with the identification of 617 as an enhancer in the central nervous system (CNS) and an allele dependent reduction of reporter gene expression, work from colleagues revealed that HCNR 617 functions as an enhancer also in the mouse animal model (Spieler D., Knauf F.). The enhancer, in this case with β-galactosidase (LacZ) as a reporter gene, was active in the forebrain of E12.5 mice and marked exclusively the embryonic ganglionic eminences (GE). The risk allele caused again a reduction of the enhancer's activity. Notably, the reporter activity overlapped with the endogenous telencephalic *Meis1* expression domain and also colocalized with transcripts of other four RLS-associated loci (PTPRD, BTBD9, MAP2K5) (unpublished data).

2.4 Putative causal variant in HCNR 617

In order to confirm the functionality of the HCNR 617 with an independent methodology electrophoretic mobility shift assays (EMSA) were conducted. Indeed, incubation of the HCNR 617 as the DNA probe with nuclear extracts from the forebrain of E12.5 mice showed two differential and specific gel shifts for the protective allele compared to the risk allele **(Figure 2.6)**. The gel shifts were specific as competition with the unlabeled allele in excess diminished the differential bands. This outcome combined with the results of the transgenic animal models, where the risk allele reduced the enhancer's function, implies an enhanced binding of an activator protein complex to the protective allele or a repressor protein complex to the risk allele of the HCNR 617. The lead SNP rs12469063 is the only variation of the DNA sequence between the two oligomers examined with EMSA. This SNP is thus responsible for the differential DNA-protein complex formation and could be classified as one of the causal SNPs for RLS.

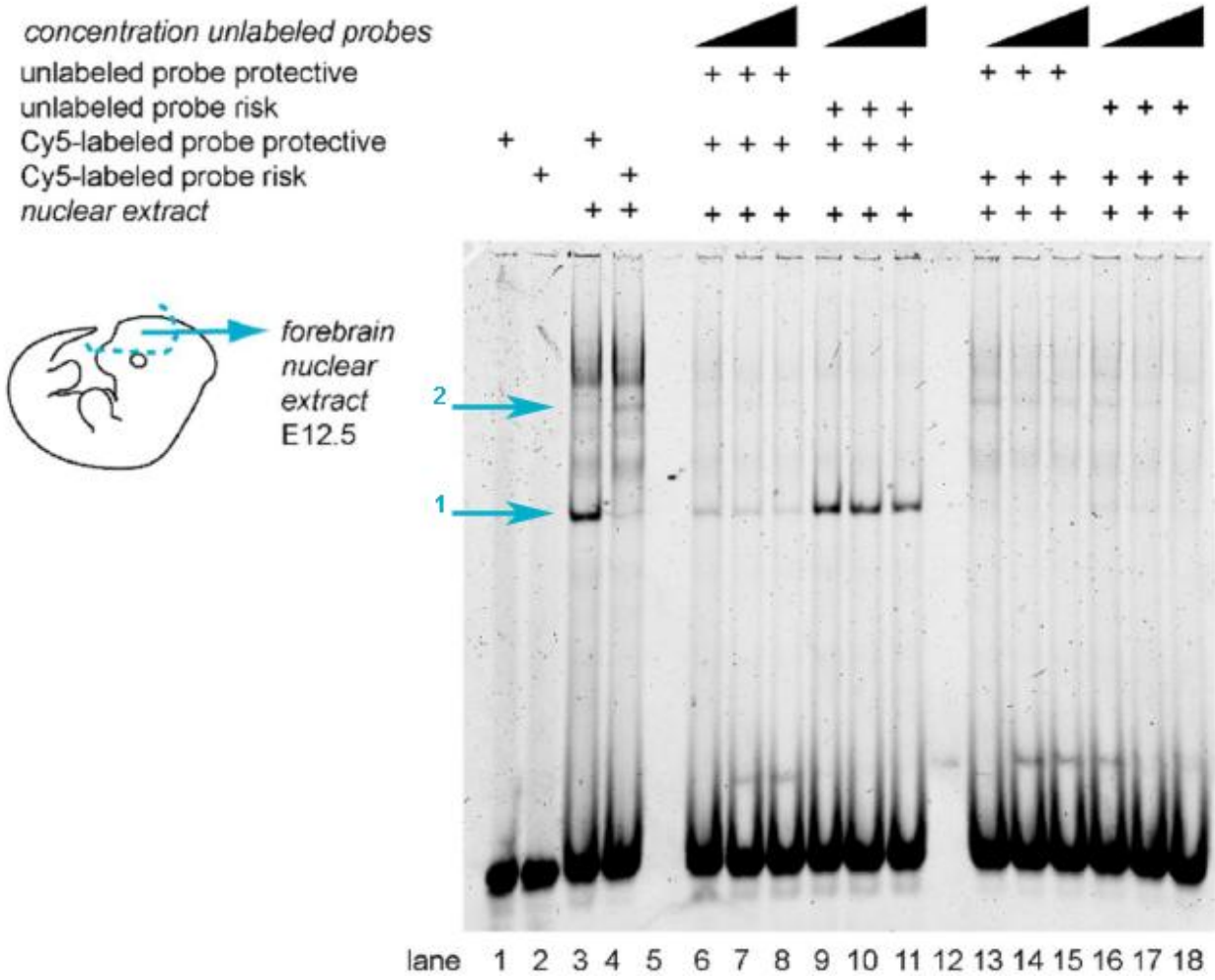

Figure 2.6. Allele-specific gel shifts for the oligomer HCNR 617 incubated with E12.5 forebrain nuclear extract

The binding of forebrain transcription factors of E12.5 embryos appears different for the protective versus the risk allele of the HCNR 617 enhancer element. The protective allele is shifted specifically after incubation with E12.5 mouse embryonic forebrain nuclear extract (lane 3, arrow 1). Incubation with the risk allele resulted in another specific band shift (lane 4, arrow 2). After competing with increasing amounts of unlabeled probes the specific DNA-protein complexes are gradually competed (lanes 6-11 and 13-18). All the other bands appearing are unspecific.

2.5 Candidate upstream factors of HCNR 617

After I demonstrated a differential and allele-dependent DNA-protein complex formation in EMSA, my next goal was to identify the proteins that bind differentially to the protective versus the risk allele of HCNR 617. The upstream factors that bind differentially to the respective allele were enriched from nuclear extracts of E12.5 mouse forebrains using affinity chromatography and identified with mass spectrometry **(Figure 2.7 and Table 2.2)**. For the affinity chromatography I used biotin-labeled oligonucleotides with the same DNA sequence for the protective and risk allele as in EMSA. The biotin-labeled oligonucleotides were incubated with nuclear extract of E12.5 mouse forebrain and streptavidin-coupled magnetic beads.

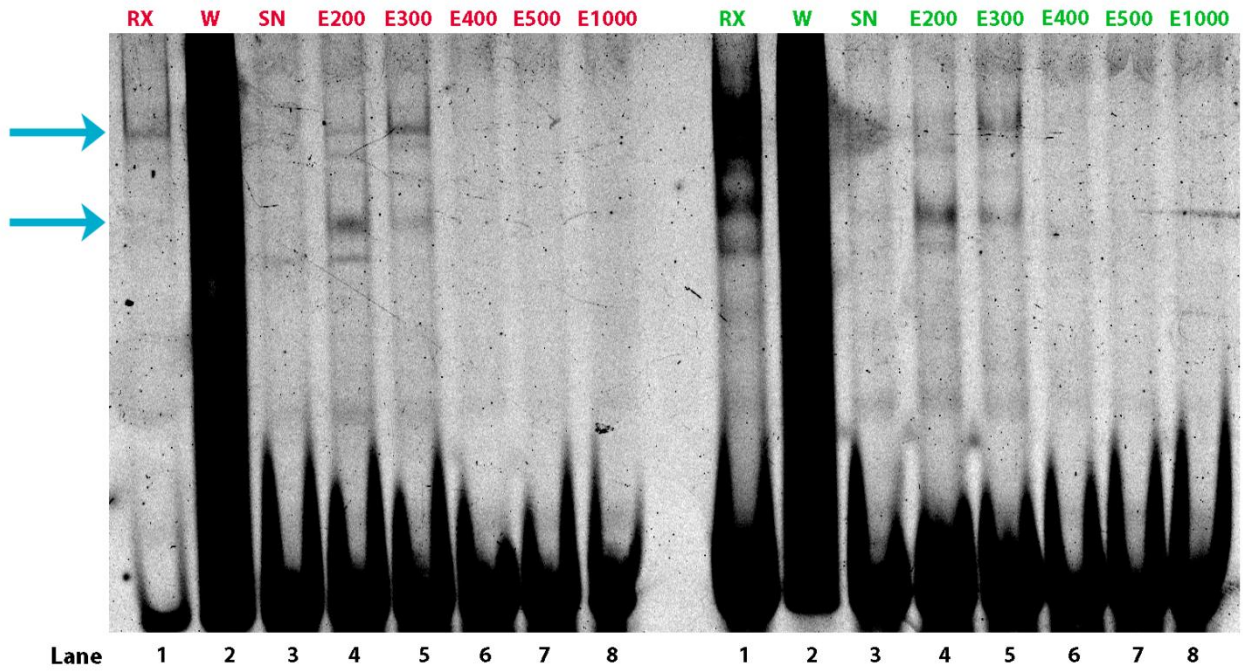

Figure 2.7. Representative EMSA gel after affinity chromatography with differentially eluted proteins depending on the HCNR 617 allele
This EMSA gel represents one of at least three EMSA gels that followed the affinity chromatography. It depicts the differentially eluted proteins (at the level of the cyan

arrows) after incubation of E12.5 forebrain nuclear extracts with the biotinylated oligomers of the HCNR 617 protective allele (green color) and risk allele (red color). The proteins were eluted using an ascending amount of salt concentration. The elution E300 that presents differential intensity on the gel comparing the two alleles has been processed for identification with mass spectrometry. RX stands for reaction, W for wash, SN for supernatant, and E for elution, with the numbers denoting the salt concentration (mM).

Protein Ids	Name	Description	Peptides used for quantitation	Max fold change	Highest mean condition	Lowest mean condition
ENSMUSP00000027097	**Creb1**	cAMP responsive element binding protein 1	1	2.2	R	NR
ENSMUSP00000021062	**Ddx5**	DEAD (Asp-Glu-Ala-Asp) box helicase 5	3	2.2	NR	R
ENSMUSP00000006625	**Rbm14**	RNA binding motif protein 14	3	2.1	NR	R
ENSMUSP00000027777	**Parp1**	poly (ADP-ribose) polymerase 1	18	2.0	NR	R
ENSMUSP00000075067	**Npm1**	nucleophosmin (nucleolar phosphoprotein B23, numatrin)	10	1.8	R	NR
ENSMUSP00000078589	**Ybx1**	Y box binding protein 1	2	1.8	R	NR
ENSMUSP00000053943	**Basp1**	brain abundant, membrane attached signal protein 1	6	1.5	R	NR
ENSMUSP00000065940	**Hmgb2**	high mobility group box 2	8	1.5	R	NR
ENSMUSP00000068896	**Top2a**	topoisomerase (DNA) II alpha 170kDa	7	1.5	NR	R

Table 2.2. Partial table of the mass spectrometry data for HCNR 617

The acquired spectra were loaded into the Progenesis LC-MS software (version 4.0, Nonlinear) for label free quantification based on peak intensities. Spectra were searched against the Ensembl mouse database (Release 62; 54576 sequences). Normalized abundances of all unique peptides were summed up and allocated to the respective protein. Normalized abundances of the experimental groups were averaged within the groups and fold changes were calculated, comparing the protective (NR) with the risk (R) condition (Max fold change). The proteins were ranked according to the fold changes from the highest to the lowest, with a cutoff of ≥1.5. For more details and the complete list of the identified proteins, see methods and appendix (Appendix: Table).

I used different selection criteria to select promising candidate proteins from the mass spectrometry data. These included an already known function and expression of the protein in developing CNS and the ability of the protein to bind DNA in a sequence-specific manner. In addition, I examined the presence of the protein's consensus motif within the DNA sequence of HCNR 617. The software suite Genomatix was used for all these analyses (GeneRanker software).

By applying the above criteria from a starting point of 63 proteins and with a cutoff of ≥1.5 fold change, I identified only seven DNA-binding proteins: Creb1, Parp1, Npm1, Ybx1, Basp1, Hmgb2 and Top2a. From these candidates only Creb1, Parp1 and Ybx1 are binding DNA in a sequence-specific manner. Thus, I selected Creb1, Parp1 and Ybx1 as promising candidates from the mass spectrometry data, based on annotation data. Creb1 and Ybx1 are expressed in the same anatomical region, where the enhancer is active and colocalize partly with *Meis1* expression **(Figure 2.8, Figure 2.9)**. Their involvement in developmental processes of the CNS and the prediction of putative binding sites on HCNR 617, using bioinformatics tools (Genomatix software suite, MatInspector tool), support further these factors as regulators of *Meis1* expression. In addition, a few known cofactors of Creb1, such as Apex1, Parp1 and of Ybx1, such as Fus, Npm1 were identified through mass spectrometry (see also **Table 2.2)**. This additional evidence from the mass spectrometry data implies that the combinatorial binding of specific transcription factors and their cofactors is important for orchestrating *Meis1* expression.

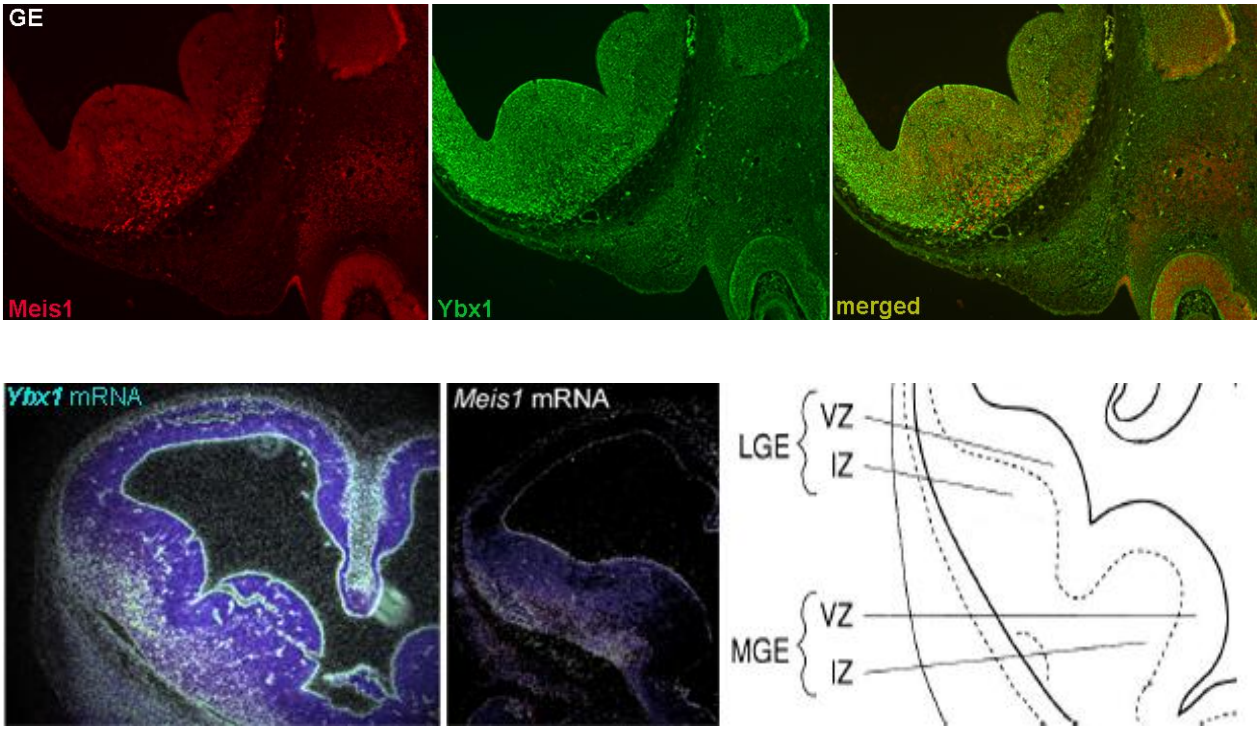

Figure 2.8. Meis1 and Ybx1 proteins and transcripts map to the ganglionic eminences of E12.5 mice

Ybx1 and Meis1 proteins (upper panel) as well as *Ybx1* and *Meis1* transcripts (lower panel) colocalize in the mantle zone of the ganglionic eminences in E12.5 mouse embryos. MGE and LGE stand for medial and lateral ganglionic eminence, respectively, with their ventricular (VZ), intermediate (IZ) and mantle zones (MZ).

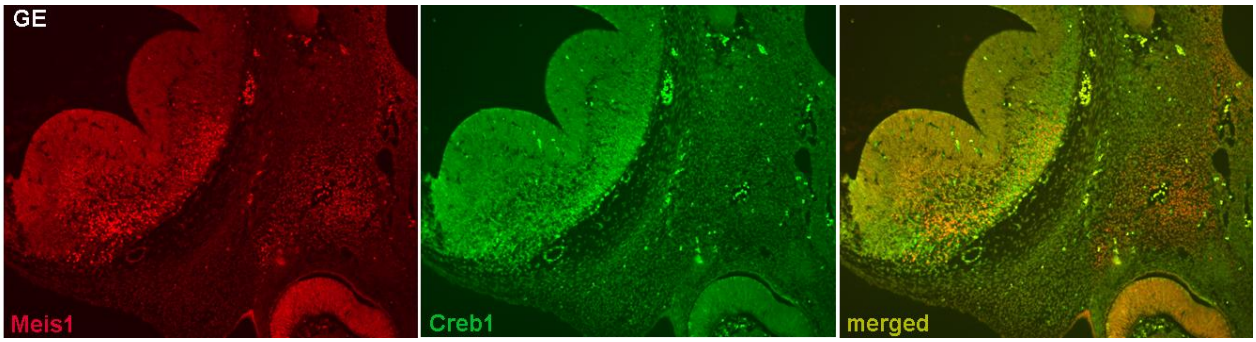

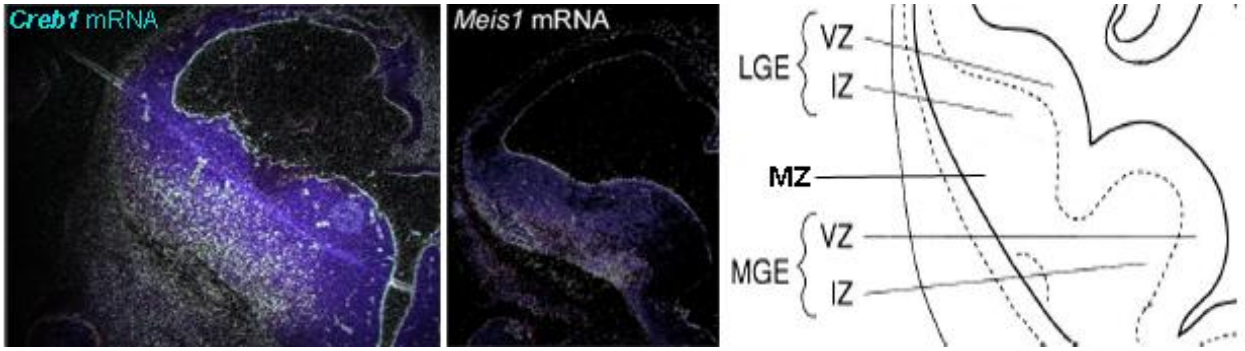

Figure 2.9. Meis1 and Creb1 protein and transcript map to the ganglionic eminences of E12.5 mice
Creb1 and Meis1 proteins (upper panel) as well as *Ybx1* and *Meis1* transcripts (lower panel) colocalize in the MZ of the ganglionic eminences in E12.5 mouse embryos.

To validate experimentally the predicted binding of Creb1 and Ybx1 on HCNR 617, I performed supershift assays, using antibodies against these proteins. The supershift assay using an antibody against Ybx1 protein almost eliminated the upper specific gel shift and revealed that this transcription factor binds preferentially to the risk allele of HCNR 617 **(Figure 2.10)**. This result is also supported by the mass spectrometry finding, where Ybx1 binds 1.8 fold more to the risk versus the protective allele. Thus, Ybx1 acts in this case as a repressor on the HCNR 617, reducing the enhancer's activity in the case of the risk allele. The anti-Creb1 antibody on the other hand did not reveal any supershift in EMSA (four different anti-Creb1 antibodies assessed). To this point no experimental data were acquired for Parp1.

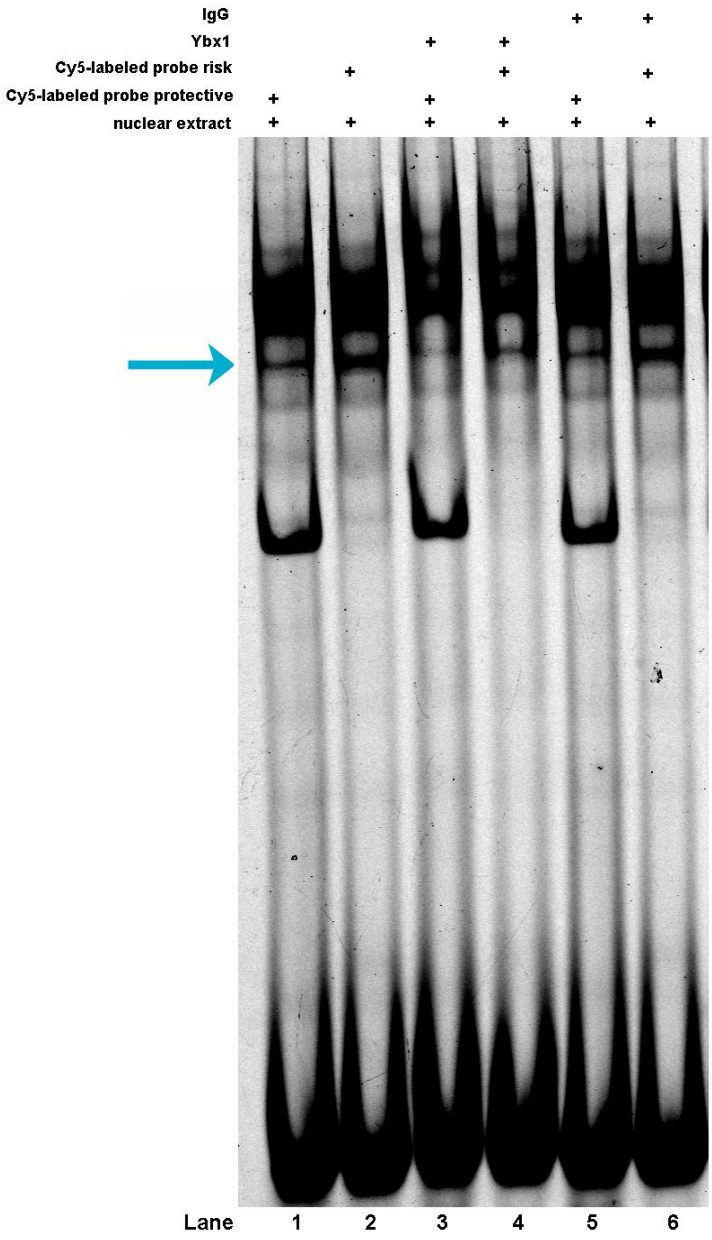

Figure 2.10. Ybx1 protein interacts with HCNR 617 in EMSA
Ybx1 protein binds stronger to the risk allele of HCNR 617 and weaker to the protective allele (lane 1 and 2, cyan arrow). With the addition of the anti-Ybx1 antibody this gel shift almost disappears, in other words the antibody competes with the Ybx1 protein for the DNA binding (lane 3 and 4). This is not the case for the antibody against the anti-IgG immunoglobulin, which is used as a negative control and shares the same isotype-species with the anti-Ybx1 antibody.

2.6 Putative causal variant in HCNR 631

In order to validate the allele-dependent difference of the functional HCNR 631 in luciferase assays, I employed EMSA using nuclear extracts of 293T cells and HCNR 631 as the labeled oligonucleotide probe. In this case, the EMSA revealed a stronger and unique binding for the risk allele compared to the protective allele **(Figure 2.11)**. As the risk allele reduced the expression of the reporter gene in luciferase assays, in other words reduced the enhancer's function, the EMSA indicates an enhanced binding of a repressor protein to the risk allele. This outcome suggests another putative causal SNP (rs62145814) for RLS residing in the HCNR 631.

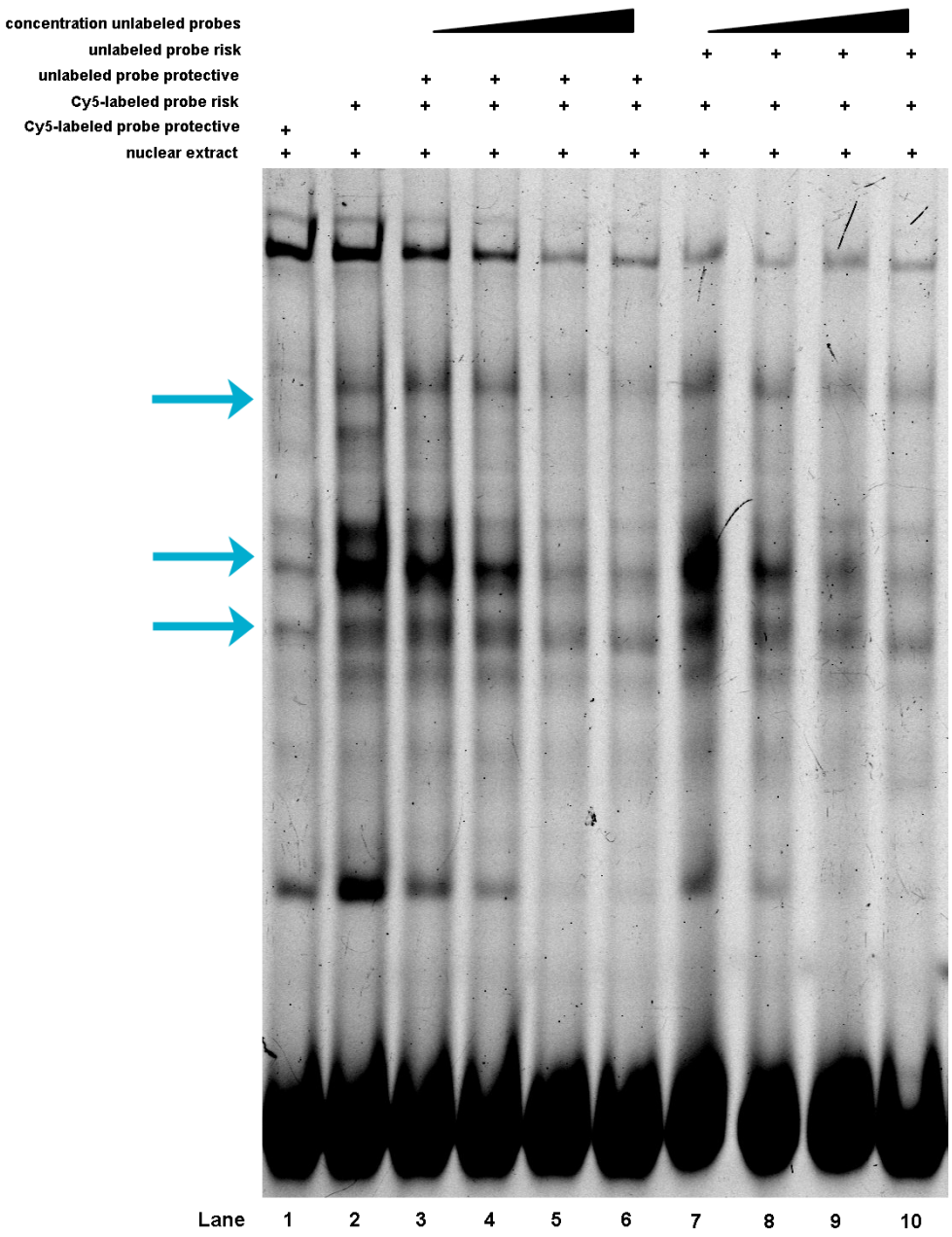

Figure 2.11. Allele-specific gel shifts for the oligomer HCNR 631 incubated with 293T nuclear extract

The differential DNA-protein specific complexes for the protective allele (lane 1) and the risk allele (lane 2) of the HCNR 631 are marked with two cyan arrows. In the case of HCNR 631 the risk allele binds stronger to nuclear proteins of 293T cells than the protective allele. In the competition assay, after competing with an increasing amount of unlabeled risk probe the specific DNA-protein complexes are gradually competed (lanes 7-10), though after competing with an increasing amount of unlabeled protective probe

the specific DNA-protein complex is less competed (lanes 3-6). All remaining bands on the EMSA gel are not specific.

2.7 Candidate upstream factors of HCNR 631

In analogy to HCNR 617, I followed the same approach for HCNR 631 to identify the upstream factors that bind differentially and may also be involved in RLS pathology. These factors were enriched from nuclear extracts of 293T cells using affinity chromatography and identified with mass spectrometry **(Figure 2.12 and Table 2.3).**

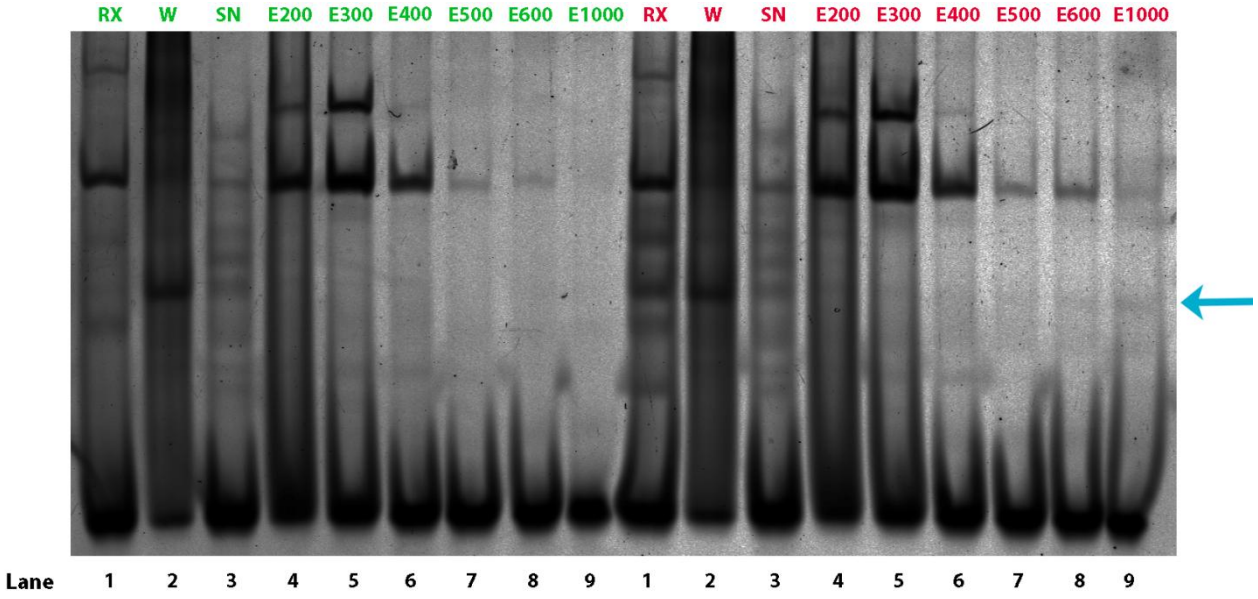

Figure 2.12. Representative EMSA gel after affinity chromatography with differentially eluted proteins depending on the HCNR 631 allele
This EMSA gel represents one of at least three EMSA gels that followed the affinity chromatography. It depicts the differentially eluted proteins (at the level of the cyan arrow) after incubation of 293T nuclear extract with the biotinylated oligomers of the HCNR 631 protective allele (green color) and risk allele (red color). The proteins were eluted using an ascending amount of salt concentration. The elution E1000 that varied in intensity on the gel, comparing the two alleles, has been processed for identification with mass spectrometry. RX stands for reaction, W for wash, SN for supernatant, and E for Elution, with the numbers denoting the salt concentration (mM).

Protein Ids	Name	Description	Peptides used for quantitation	Max fold change	Highest mean condition	Lowest mean condition
ENSP00000066544	CDC27	cell division cycle 27 homolog (S. cerevisiae)	1	70.4	R	NR
ENSP00000370808	SLC25A6	solute carrier family 25 (mitochondrial carrier; adenine nucleotide translocator), member 6	1	14.8	R	NR
ENSP00000373370	FLG2	filaggrin family member 2	2	6.8	R	NR
ENSP00000340889	PRSS3	protease, serine, 3	1	5.7	R	NR
ENSP00000310275	BANF1	barrier to autointegration factor 1	1	3.6	R	NR
ENSP00000240361	TEX14	testis expressed 14	1	3.5	R	NR
ENSP00000353132	**DMBX1**	**diencephalon/mesencephalon homeobox 1**	**1**	**3.1**	**NR**	**R**
ENSP00000262746	PRDX1	peroxiredoxin 1	1	3.1	R	NR
ENSP00000259726	CDSN	corneodesmosin	1	2.8	R	NR
ENSP00000296736	TIGD6	tigger transposable element derived 6	1	2.2	NR	R
ENSP00000291009	PIP	prolactin-induced protein	1	2.2	R	NR
ENSP00000344903	MAFK	v-maf musculoaponeurotic fibrosarcoma oncogene homolog K (avian)	1	2.1	R	NR
ENSP00000380352	DDHD2	DDHD domain containing 2	1	2.0	R	NR
ENSP00000217182	EEF1A2	eukaryotic translation elongation factor 1 alpha 2	1	1.9	R	NR
ENSP00000308485	PDE4D	phosphodiesterase 4D, cAMP-specific	1	1.8	NR	R
ENSP00000346694	HNRNPA2B1	heterogeneous nuclear ribonucleoprotein A2/B1	1	1.8	R	NR
ENSP00000319690	HNRNPC	heterogeneous nuclear ribonucleoprotein C (C1/C2)	3	1.8	R	NR
ENSP00000257192	DSG1	desmoglein 1	2	1.8	R	NR
ENSP00000355759	**PARP1**	**poly (ADP-ribose) polymerase 1**	**54**	**1.8**	**R**	**NR**
ENSP00000254108	FUS	fused in sarcoma	1	1.7	R	NR
ENSP00000237172	FILIP1	filamin A interacting protein 1	1	1.7	NR	R
ENSP00000261366	LMNB1	lamin B1	3	1.6	R	NR
ENSP00000084795	RPL18	ribosomal protein L18	1	1.6	R	NR
ENSP00000331514	ACTG1	actin, gamma 1	4	1.6	R	NR
ENSP00000354876	MT-CO2|	mitochondrially encoded cytochrome c oxidase II	1	1.5	NR	R
ENSP00000340251	TMPO	thymopoietin	2	1.5	R	NR

Table 2.3. Table of the mass spectrometry data for HCNR 631

The acquired spectra were loaded into the Progenesis LC-MS software (version 4.0, Nonlinear) for label free quantification based on peak intensities. Spectra were searched against the Ensembl human database (Release 66, 96556 sequences). Normalized abundances of all unique peptides were summed up and allocated to the respective protein. Normalized abundances of the experimental groups were averaged within the groups and fold changes were calculated, comparing the protective (NR) with the risk (R) condition (Max fold change). The proteins were ranked according to the fold changes from the highest to the lowest, with a cutoff of ≥1.5. For more details, see methods.

In order to identify promising candidate proteins from the mass spectrometry data I used the same selection criteria as for HCNR 617. These included an already known function and expression of the protein in developing CNS and the ability of the protein to bind DNA in a sequence-specific manner. The software suite Genomatix was used again for all these analyses (GeneRanker software). Following this approach, from 26 identified proteins and with a cutoff of ≥1.5 fold change, the diencephalon/mesencephalon homeobox 1 or orthodenticle homeobox 3 (DMBX1/OTX3), Poly (ADP-ribose) polymerase 1 (PARP1) and v-maf avian musculoaponeurotic fibrosarcoma oncogene homolog K (MAFK) emerged as a possible candidates. Although OTX3 demonstrated a stronger binding to the protective allele according to mass spectrometry, it colocalized partly with *Meis1* expression in the caudal ganglionic eminence of E12.5 mouse embryos **(Figure 2.13)** and is required for brain development (see Discussion). At this point, no experimental data were obtained for PARP1 and MAFK. The high mobility group nucleosome binding domain 1 (HMGN1), fused in sarcoma (FUS) and complement component 1, q subcomponent binding protein (C1QBP) were annotated as transcriptional cofactors that bind DNA unspecifically (GeneRanker software).

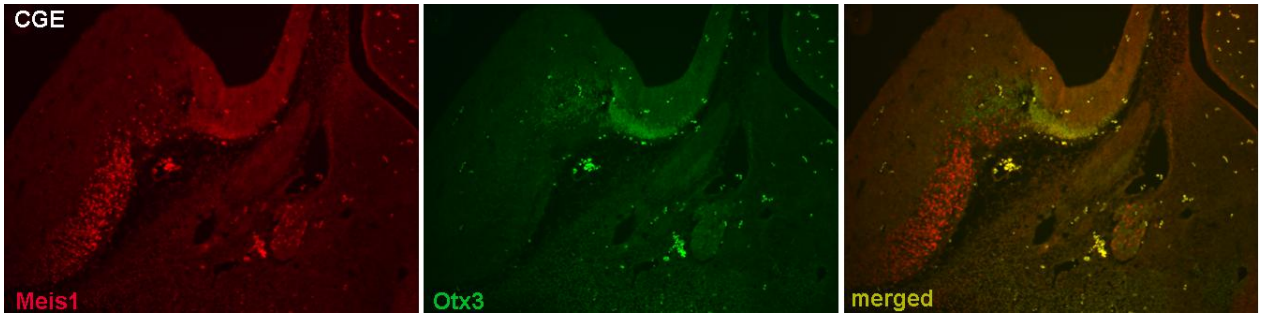

Figure 2.13. Meis1 and Otx3 protein map to the caudal ganglionic eminence of E12.5 mice
Otx3 and Meis1 proteins are detected in the caudal ganglionic eminence (CGE) of E12.5 mouse embryos.

In addition, I performed supershift assays to demonstrate experimentally a putative binding of OTX3 on HCNR 631. However, supershift assays examining two different antibodies against OTX3 did not reveal any positive supershift.

3 DISCUSSION

3.1 Summary

In summary during my doctoral work I explored and identified the link between the intronic RLS association signal within *MEIS1* and its functional correlate. *MEIS1* is a highly conserved developmental gene with a homeobox domain. Through screening for conservation six HCNRs with RLS-associated variants, were identified in the RLS-associated 32 kb LD block.

I have demonstrated that all six HCNRs are functional in a cellular system, in other words function as enhancers or silencers, by performing dual luciferase assays in 293T cell lines with various effect sizes depending on the construct. An allele-specific difference in reporter assays was demonstrated for two of them, HCNR 617 and HCNR 631, implying relevance of the associated SNPs for the RLS phenotype. HCNR 617 functioned as a silencer in various cell lines, including two neuroblastoma cell lines and as an enhancer in mouse and zebrafish animal models, with the risk allele reducing the enhancer's activity (unpublished data). HCNR 631 functioned as enhancer in 293T cell line with the risk allele again reducing the enhancer's activity.

EMSA verified for both HCNRs (617 and 631) the differential formation of DNA-protein complexes, depending on the allele (protective or risk allele). Finally, affinity chromatography combined with mass spectrometry analysis pinpointed upstream factors that bind allele-specific and differentially. In the case of HCNR 617, top candidates were Creb1 and Ybx1 that colocalized with Meis1 in ganglionic eminences of E12.5 mice (both at the level of protein and mRNA). Both proteins bind the DNA sequence of

HCNR 617 according to bioinformatic analysis (Genomatix software suite, MatInspector tool).

Furthermore, anti-Ybx1 antibody displayed a supershift of the specific gel shift. For HCNR 631 a top candidate was OTX3/DMBX1, after the analysis of the mass spectrometry data. Otx3 is also expressed in the caudal ganglionic eminences of E12.5 mice like Meis1.

In conclusion, I demonstrated that the intronic association signal of *MEIS1* for RLS accommodates functional highly conserved elements. These *cis*-regulatory elements carry variants that bind transcription factors differentially and contribute to the regulation of *MEIS1* expression.

3.2 Function derived from a genome wide signal

The functionality underlying genome wide association signals that has been revealed through this work demonstrates the importance of conserved non-coding elements in regulating the expression of genes. In the era of ENCODE project, which aims to identify all functional elements of the human genome, this work demonstrates an effective way to reveal the signal transduction pathways that play a role in the pathophysiology of a disease. Initiated from human genetics, where RLS was associated with DNA variants (SNPs) and consecutively employing a variety of functional studies I was able to unravel at least three unknown proteins (YBX1, CREB1, and OTX3) that are possibly involved in RLS pathology.

3.2.1 YBX1

In more detail YBX1, belongs to a family of highly evolutionary conserved proteins that bind specifically to Y-box (5'-CTGATTGGCCAA-3') regulatory elements of genes, such as the human leukocyte antigen (HLA) class II genes. The Y-box proteins contain “cold shock” domains (CSD) that exhibit a broad spectrum of nucleic-acid binding properties, an attribute promoting their large repertoire of functions in cytoplasm and nucleus (Braun, 2000; Wilkinson et al., 2001; Kohno et al., 2003). They shuttle between the cytoplasmic and nuclear compartments in response to physiological and environmental cues (Faustino et al., 2003; Raffetseder et al., 2003). Within nucleus Ybx1 functions as transcription factor and regulates the transcription of many genes. It is also implicated in DNA repair and pre-mRNA alternative splicing and transport, by binding to splice sites (Faustino et al., 2003; Kohno et al., 2003). Ybx1 in cytoplasm binds and stabilizes cytoplasmic mRNA and regulates protein synthesis, by modulating the interaction between the mRNA and initiation factors (Matsumoto et al., 1998; Swamynathan et al., 1998; Evdokimova et al., 2001; Bader et al., 2005). Thus, CSD proteins have been proposed to function as multifunctional coordinators for the control of gene expression in both the nucleus and cytoplasm (Wilkinson et al., 2001; Kohno et al., 2003).

YBX1 is overexpressed in malignant tissues, such as breast cancer, non-small cell lung cancer, ovarian serous adenocarcinomas, human osteosarcomas, colorectal carcinomas and malignant melanomas (Bargou et al., 1997; Oda et al., 1998; Kamura et al., 1999; Shibao et al., 1999; Hipfel et al., 2000; Shibahara et al., 2001) . In the case of breast cancer it is responsible for the up-regulation of MDR1 gene, resulting in a multidrug resistant phenotype and lower survival rates. Ybx1 functions as a cell cycle regulator,

important for cell proliferation both in development and malignant diseases (Jurchott et al., 2003). Its secreted form acts as an extracellular mitogen and stimulates cell migration and proliferation (Frye et al., 2009).

The Ybx1 knock-out mouse embryos are embryonic lethal (between E14.5 and E18.5) and exhibit exencephaly associated with abnormal patterns of cell proliferation within the neuroepithelium (Uchiumi et al., 2006). These results demonstrate that Ybx1 is involved in early mouse development, including neural tube closure and cell proliferation, a fact also relevant in our case.

3.2.2 CREB1

CREB1 is a transcription factor and member of the leucine zipper family of DNA binding proteins. This protein is activated by phosphorylation by several protein kinases, binds as a homodimer to the cAMP-responsive element (CRE, an octameric palindrome) and induces transcription of genes in response to hormonal stimulation of the cAMP pathway (Berkowitz et al., 1990; Matthews et al., 1994). CREB protein exhibits different roles depending on the brain region involved. Activation of Creb in the hippocampus is linked to the therapeutic efficacy of antidepressant treatments. On the other hand, activation of Creb in the nucleus accumbens, amygdala and several other regions by drugs of abuse or stress mediates drug addiction, depressive and anxiety-like behaviors (Carlezon et al., 2005). Striatal Creb1 regulates sensitivity and therefore behavioral responses to psychostimulants (Madsen et al., 2012). Binding of Creb to the CRE element of human BDNF gene is critical for activity-dependent functions on the CNS, something that is dysregulated in various neuropsychiatric disorders (Pruunsild et al., 2011). CREB signaling is a central pathway in adult hippocampal neurogenesis, synaptic plasticity,

intrinsic excitability, playing an important role in learning and memory (Jagasia et al., 2009; Barco et al., 2011).

Mice with Crem$^{-/-}$ (cAMP response element modulatory protein) background that also lack Creb1 in the CNS during development show extensive apoptosis of postmitotic neurons. However, mice lacking both Creb1 and Crem in the postnatal forebrain show progressive neurodegeneration in the hippocampus and in the dorsolateral striatum, with a phenotype reminiscent of Huntington disease (Mantamadiotis et al., 2002).

Creb is also involved in synchronization of circadian rhythmicity. Notably the CRE transcriptional pathway is responsible for both the maintenance of suprachiasmatic nucleus timing and light entrainment of the circadian clock (Lee et al., 2010). This is of great interest as the RLS phenotype possesses also a circadian component, with exacerbation of the symptoms at the late evening/night (Walters, 1995; Allen et al., 2003b). Last but not least, it is known that Creb regulates *Meis1* expression in normal and malignant hematopoietic cells (Esparza et al., 2008) and binds to the MEIS1A and MEIS1B C termini (Huang et al., 2005). This data support my finding that Creb1 is one of the factors that bind upstream of the HCNR 617.

3.2.3 OTX3/DMBX1

OTX3 is the newest member of paired class homeodomain transcription factors, first identified in 2002 (Ohtoshi et al., 2002; Zhang et al., 2002). For this reason not much is known about this member of the bicoid sub-family of homeodomain transcription factors. It is expressed in the developing brain, eyes, forelimb and hindlimb, and the adult cerebellum in mice (Ohtoshi et al., 2002; Zhang et al., 2002). An expression pattern that is very similar to the Meis1 homeobox protein. The Otx3 knockout mice exhibit neonatal

lethality, dwarfism and abnormal brain morphology, suggesting an important role in brain development (Ohtoshi et al., 2004). Those mice that survive to adulthood predominantly display hypophagia and hyperactivity, likely as a result of defects in the development of the neural circuitry involved in energy homeostasis (Fujimoto et al., 2007). Hyperactivity is a relevant feature for RLS. Duplicate dmbx1 genes regulate progenitor cell cycle and differentiation during zebrafish midbrain and retinal development (Wong et al., 2010). In conclusion, Otx3 functions as a transcriptional repressor and represses Otx2-mediated transactivation by forming a heterodimer with Otx2.

At this point it is important to mention that few cofactors of Creb1 and Ybx1 such as Apex1, Parp1 and Fus, Npm1, respectively were identified with our mass spectrometry approach, which further supports the reliability of the data.

This is additional evidence that the identified proteins are working in a network that may be RLS relevant, taking into account the differential DNA-protein complex formation between the two RLS-associated alleles.

3.3 Perspectives

3.3.1 Function of the RLS-associated HCNR 617 (lead SNP)

The HCNR 617 functioned as a silencer in all six cell lines (293T, HEK293, HeLa, COS-7, SHSY-5Y and IMR32) examined, but as an enhancer in the CNS of the animal models (zebrafish and mouse). This may appear contradictory, but it is possible that this region functions as a regulatory element in a tissue specific manner. In other words, HCNR 617 can function by enhancing transcription in specific anatomical regions of CNS, or by silencing transcription in other anatomical regions, depending on the factors and cofactors that bind upstream to this element and can be coactivators or

corepressors. An activator can switch to a repressor by differential cofactor binding. An example of this is the work by Perissi et al. that demonstrated a switch from gene repression to gene activation by the alternating function (once as corepressors and once as coactivators) of TBL1/TBLR1 factors (Perissi et al., 2004). Often *cis*-regulatory elements that are active in development function in a restricted spatiotemporal fashion. That means those are active for a specific time frame and marking a specific tissue and become silent in every other case. In other words, if the HCNR 617 acts as a mouse forebrain-specific enhancer during development (E12.5), it will remain silent in every cell line that does not exhibit the regulatory network of forebrain at E12.5.

3.3.2 Function of the remaining RLS-associated HCNRs

To reveal the *cis*-regulatory architecture of *MEIS1* I employed cell-based luciferase assays, based on DNA sequence conservation. However, as a cell-based assay is an artificial *in-vitro* system, which only resembles partially the *in-vivo* environment, colleagues in my laboratory used reporter assays in the zebrafish and mouse animal model. With the animal models we tried to approach closer the human physiology. Still, our findings may not apply entirely to humans, as humans acquired also their own lineage-specific, often poorly conserved regulatory elements through evolution.

Besides HCNR 617, the zebrafish screen identified HCNR 629 and HCNR 631 as *cis*-regulatory elements that showed neural, allele-dependent reporter activity. However the reporter activity was spatially not reproducible, as if boosting the position effects and is previously referred as booster activity (Royo et al., 2012). Additional functional HCNRs in the RLS-associated 32 kb LD block might explain the risk haplotype, defined by

rs6710341/rs12469063. The haplotype increases the OR and underlines the existence of more functional variants besides the lead SNP rs12469063 within the MEIS1 locus.

Additionally in the zebrafish screen, the HCNR 602 also showed a reporter activity without any spatially reproducible pattern. The HCNR 622 functioned as an enhancer in hematopoietic stem cells and the HCNR 606 functioned as a midbrain enhancer. These results in the zebrafish animal model come to further support the results of the dual luciferase experiments in cell lines, where the above elements functioned also as *cis*-regulatory elements.

3.3.3 Functional HCNRs encompassing putative causal variants

During this work I followed only functional HCNRs comprising RLS-associated SNPs that showed an allele-specific difference in the reporter assays. The remaining HCNRs, which I have demonstrated to be functional in a cell-based luciferase assay, may demonstrate an allele-specific effect on gene regulation in particular tissues and may play a role in other phenotypes-diseases. An example is the case of HCNR 606, which I used as a control, as it does not include any RLS-associated SNP. This HCNR functioned as an enhancer, with the risk allele reducing the enhancer's activity and probably this variant is relevant for another phenotype. In addition, a genome wide association study associated a variant, rs11897119 that lies in the HCNR 622 of *MEIS1* with elongated electrocardiographic PR interval (Pfeufer et al., 2010). This SNP does not reach the level of genome wide significance in our RLS association study and probably plays no role in RLS, but has a putative role as PR interval modifier.

3.3.4 Knockout animal models of great importance for RLS

Loss of the Drosophila homolog of BTBD9 gene (dBTBD9) disrupts sleep in flies, with increased waking and motor activity (Freeman et al., 2012). The authors showed also that *dBTBD9* regulates brain dopamine levels in flies and controls iron homeostasis in human cell lines. Thus, the phenotype in flies could be parallelized with the RLS phenotype. The loss-of-function model of the Btbd9 gene in mouse demonstrated motor restlessness, sensory alterations likely limited to the rest phase, decreased sleep and increased wake times during the rest phase. Additionally, the Btbd9 mutant mice had altered serum iron levels and their sensory alterations were relieved using ropinirole, a dopaminergic agonist widely used for RLS treatment (DeAndrade et al., 2012).

At present, only one knockout mouse model for Meis1 has been reported, but the researchers of that study focused on the hematopoiesis and vascular patterning without examining the CNS (Azcoitia et al., 2005). The mutant mice in our screening showed increased locomotion in open field test, especially the last hours before sleep, and an abnormal acoustic startle reflex, which denotes a motor gating deficit (unpublished data, in collaboration with the German Mouse Clinic, Helmholtz Zentrum München). These observations are of great importance as the RLS phenotype incorporates restlessness, primarily the late evening and night. Taking this data into account, I could argue that part of the pathology of RLS could be explained from the dysregulation of *Meis1* expression. RLS-relevant differences in the regulation of downstream target genes of *Meis1* will be elucidated by performing ChIP-Seq analysis in the developing forebrain and identifying the downstream targets of *Meis1* that could be affected.

3.3.5 RLS and basal ganglia

In parallel to my work other colleagues in the laboratory worked with zebrafish and mouse animal models and demonstrated allele-dependent differential enhancer function for HCNR 617 of MEIS1 gene in the embryonic ganglionic eminences of the developing forebrain (Spieler D., Knauf F. et al., unpublished data). This data supports the notion that at least one region involved in RLS pathology is the basal ganglia that develop from the ganglionic eminences. It also highlights a developmental component for RLS. As aging is a risk factor for RLS, this may mean that early developmental changes in gene regulation might not be compensated at later stages in adult life (Somel et al., 2010). As discussed also in the introduction there is considerable evidence that links RLS to basal ganglia. The D2R is decreased in putamen of RLS patients and correlates also with RLS severity (Connor et al., 2009). DAT showed decreased binding in the striatum (putamen and caudate) of RLS patients (Earley et al., 2011). Several studies have shown a reduction of D2 receptor occupancy in the striatum of RLS patients (Staedt et al., 1993; Staedt et al., 1995; Staedt et al., 1995; Michaud et al., 2002; Tribl et al., 2004). Furthermore, the iron level is decreased in the caudate head and thalamus of idiopathic RLS patients (Godau et al., 2008). At last, unmedicated patients with early onset RLS showed increased iron content in globus pallidus internal and subthalamic nucleus, suggesting a dysfunction of the basal ganglia (Margariti et al., 2012). All this data support the notion that dysfunction of the basal ganglia is correlated with RLS.

3.3.6 Future plans

3.3.6.1 Upstream factors regulating MEIS1 expression

To overcome the technical difficulties of the supershift assays and to examine, if Ybx1, Creb1, and Otx3 proteins indeed regulate the expression of HCNR 617 and HCNR 631, respectively with a different *in-vitro* approach, these proteins are currently overexpressed transiently in 293T cell line and dual luciferase assays are performed (ongoing experiments). An impact of the overexpressed factor on the relative luciferase expression driven by the *cis*-regulatory element (HCNR 617 and 631) will suggest that this factor regulates the expression of the HCNR.

I also identified a second specific gel shift in EMSA (lower band, arrow 1 in Figure 2.6) for HCNR 617 that gives evidence for a second DNA-protein complex formation specific for the protective allele. The upstream factors that form this complex possibly function as activators of the enhancer. Only Parp1 was enriched 2.2 fold after incubation with the protective allele in comparison with the risk allele, after relative quantification with mass spectrometry.

Future work will also focus on the remaining transcription factors identified by mass spectrometry; such as PARP1 (for both HCNR 617 and HCNR 631) and MAFK (for HCNR 631). I will take into account the function of every candidate, the area of its expression and genome wide association data for RLS. In this fashion, I will acquire a better view of the regulatory pathway of *MEIS1* and its implication in RLS and other diseases.

3.3.6.2 Revealing the landscape of Meis1 genome wide binding

As *Meis1* expression seems to be compromised in RLS patients the identification of Meis1 downstream targets will reveal putative factors that their expressional imbalance leads to RLS. Toward this direction, I performed ChIP of Meis1 combined with high throughput sequencing, using forebrain tissue of E12.5 mice embryos. This work is still in progress (analysis of the ChIP-Seq data) and will reveal a spectrum of genes that are regulated from Meis1 homeobox transcription factor. Our first approach will be to identify the genes that appear also in our genome wide association study and could contribute with *MEIS1* to the RLS phenotype. In conclusion, the identification of additional factors that are compromised in RLS will lead to a better understanding of the disease and to a more targeted treatment.

3.4 General discussion

The six functional RLS-associated HCNRs of *MEIS1* may act synergistically in regulating the expression of this gene, featuring its *cis*-regulatory architecture. These regulatory elements putatively loose or gain function at the individuals that are carriers of a risk haplotype, leading to an altered MEIS1 expression, probably a downregulation (Xiong et al., 2009). This loss or gain of function is apparently caused from the differential upstream factor binding to one versus the other allele. This could partially and in a small extend explain the pathology of RLS for the individuals that carry a risk haplotype in *MEIS1*, as the common variants associated with RLS contribute only weakly to the disease phenotype. However, as RLS is a complex trait with a multifactorial background there are many other factors both genetic and environmental that are implicated in its onset. Regarding the genetics of RLS, it is possible that all genes (*MEIS1*, *BTBD9*,

PTPRD9, *TOX3* and *LBXCOR1-MAP2K5*) identified in GWA studies are working in a coordinating fashion, interacting with each other and predispose with their common variants only weakly to the disease, when their relationship turns unbalanced. Evidence of this is the mutual expression pattern of these genes, at least in the developing mouse brain (Spieler D., unpublished data). This network of developmental genes may function in dopamine-related areas and regulate iron homeostasis in CNS, bringing together many implicated pathomechanisms of RLS. In addition, the identification of rare variants contributing strongly to the phenotype may unravel new genes with high effect sizes. By employing next generation high throughput sequencing we are now able to reveal rare variants that could explain the missing heritability of RLS and shed light upon RLS pathophysiology.

4 METHODS

4.1 Bioinformatics

The HCNRs to be examined were selected using the VISTA Browser v2.0 (http://pipeline.lbl.gov/cgi-bin/gateway2). We performed sequence comparisons between human (March 2006; hg18), mouse (Jul. 2007; mm9), chicken (May 2006; galGaL3), frog (Xenopus tropicalis v4.1) and pufferfish (Takifugu rubripes v4.0) with default settings (≥ 70% sequence identity in 100 bp). HCNR peaks were defined as one HCNR block when the conservation in mouse was continuous and the corresponding peaks in the chicken conservation were closer than 700 bp.

Matinspector software (Genomatix software suite) and tess software (free online tool) were employed to predict putative binding sites of transcription factors (Cartharius et al., 2005). GeneRanker software (Genomatix software suite) was used for characterization of large sets of genes by making use of annotation data from various sources, like Gene Ontology or Genomatix proprietary annotation (Berriz et al., 2003).

4.2 Generation of HCNR vectors

The highly conserved non-coding regions were amplified from human DNA of previously genotyped RLS patients and healthy probands. No rare variants with a MAF smaller than 5% were included. For each HCNR two constructs were cloned, carrying the protective or risk alleles of the associated SNPs, that means the protective or risk haplotype, respectively. To increase amplification accuracy, I used Phusion Hot Start II High-Fidelity DNA Polymerase (Thermo Scientific).

The following primers were used. In brackets is the length of the PCR product and in italics the BglI recognition site:

602_F: 5'-*tttgcctaactggc*AAACCTTCTAACACAGAATTTAGCTC and

602_R: 5'-*tttgccgccgaggc*TGCCACATTTGAATGCTACTTTAC (2375 bp),

606_F: 5'-*tttgcctaactggc*TGTATTCCCACTGCCTTGTG and

606_R: 5'-*tttgccgccgaggc*AAAGGCATGACTCTGATGAGG (1429 bp),

612_F: 5'-*tttgcctaactggc*TGTGAAGTCTCTGTTTAAATAGGAAGG and

612_R: 5'-*tttgccgccgaggc*ATTTGATGGCAGGATTTTGG (1601 bp),

617_F: 5'-*tttgcctaactggc*AATGCATAAAAAGTGGGCATT and

617_R: 5'-*tttgccgccgaggc*ACGCCATTTTGGAATGAGTC (944 bp),

622_F: 5'-*tttgcctaactggc*ACTGGCAACTTCTTTTAACTGC and

622_R: 5'-*tttgccgccgaggc*TTGCATGCCTGTTTATGAGC (3507 bp),

629_F: 5'-*tttgcctaactggc*TCCTTTATAAGTTGACAATTTTATGC and

629_R: 5'-*tttgccgccgaggc*GCTCTCCGGCAGAGACTGT (1766 bp),

631_F: 5'-*tttgcctaactggc*CCAGGCTGGTCTCTAACTCC and

631_R: 5'-*tttgccgccgaggc*TCTCCTCTTTTGCCTTTCTCC (Metabion International AG)

The PCR products were cloned at the BglI binding site, upstream of the reporter gene in the pGL4.23[*luc2*/minP] vector (Promega). Every construct carrying the protective or the risk alleles/haplotype was confirmed by sequencing with the BigDye Terminator Cycle sequencing kit (Applied Biosystems). Sequence analysis was performed using the Staden package. Previously, the gateway-cloning system (Invitrogen) has been applied, using site-specific recombination to insert the desired elements (HCNRs) in the Topo

vector. A statistically significant effect of non-relevant structural vector's elements (attR sites) on the expression of the reporter gene was detected. Consequently, we cloned the vectors using appropriate restriction endonuclease recognition sites. The cloning site of the constructs, 5' (BglI binding site) or 3' (BamHI binding site) of the reporter gene was also examined. The first construct to be tested showed a higher expression of the reporter gene, when cloned 5' of the reporter gene. Subsequently, all the remaining constructs were also cloned 5' prime of the reporter gene. The pGL4.74[*hRluc*/TK] vector was used as an internal control to normalize for the transfection efficiency (Promega).

4.3 Cell culture

293T and COS-7 cell lines were maintained in DMEM (Life Technologies) with 10% heat inactivated FBS (Sigma) and 0.5% Penicillin-Streptomycin (Invitrogen). HEK293 and SHSY-5Y cell lines were maintained in DMEM (Life Technologies) with 15% FBS (Sigma) and 0.5% Penicillin-Streptomycin (Invitrogen). IMR32 cell line was maintained in RPMI 1640 (Life Technologies) with 20% heat inactivated FBS (Sigma), 0.5% Penicillin-Streptomycin (Invitrogen) and non-essential amino acids (Life Technologies). At last, HeLa cell line was maintained in RPMI 1640 (Life Technologies) with 10% FBS (Sigma) and 0.5% Penicillin-Streptomycin (Invitrogen). All cell lines were incubated at 37 °C and 5% CO_2.

4.4 Dual luciferase reporter assays

60-80% confluent cells were seeded per well of a 24-well plate and transfected after 24 hours with 0.2-1 μg of the reporter vector (pGL4.23[luc2/minP] Vector), carrying the

putative regulatory element, and 0.1-1 ng of the pGL4.74[hRluc/TK] vector, depending on the cell line and using as a transfection reagent Lipofectamine 2000 (Invitrogen). The pGL4.74[hRluc/TK] vector was used to normalize for the transfection efficiency. The empty pGL4.23[luc2/minP] vector without any insert was used as control to indicate the baseline activity. The total amount and volume of the transfected DNA was kept constant throughout all the experiments and every cell line was examined with at least six technical replicates at three independent experiments. 24 hours after transfection the cells were lysed and the dual luciferase assays were performed according to the manufacturer's instructions (Promega). The RLUs were calculated by dividing the firefly luciferase value with the renilla luciferase control value, after subtracting the background luminescence.

4.5 Statistical analysis

The data from luciferase reporter assays were analyzed statistically by using the R programming language. The value of expression for the empty vector without any insert was set to one. Wilcoxon rank sum test was used to compare the expression of every construct (protective versus risk allele versus control reporter vector without insert), with the level of significance set at $p<0.05$, correcting every time for multiple testing.

4.6 Electrophoretic mobility shift assay

Nuclear extracts from 293T cells were prepared based on a method already published (Schreiber et al., 1989). Initially, 1-2 x 10^6 cells were washed twice on ice with 10 ml PBS and collected in 2 ml buffer A (10 mM HEPES pH 8; 10 mM KCl; 0.1 mM EDTA; 0.1 mM EGTA; 1 mM DTT; 0.5 mM PMSF). The cells were allowed to swell in the hypotonic

buffer for 15 min, and then 125 µl of 10% Nonidet NP-40 was added, followed by vortexing. The homogenate was centrifuged for 3 min at 14000 rpm. The supernatant containing the cytoplasmatic fraction was stored at -80 °C. The nuclear pellet was washed twice with buffer A, resuspended in buffer C (20 mM HEPES pH 7.9; 0.4 M NaCl; 1 mM EDTA; 1 mM EGTA; 1 mM DTT; 1 mM PMSF) and incubated for 15 min on a shaking platform. The nuclear fraction was recovered by centrifugation at maximum speed for 5 min. All the steps have been performed on ice or at 4 °C. Nuclear extracts were also prepared from dissected forebrains of E12.5 mouse embryos using NE-PER Nuclear and Cytoplasmic Extraction Reagents (Thermo Fisher Scientific). *Meis1* expression domains adjacent to the identified telencephalic area in the ganglionic eminences, such as mandible, maxilla and eye were carefully removed.

The sequence of the oligomers for the protective alleles was:

617_F: 5'-cy5-GCTTCCAGCTGTGGCAGGCATGATGCAGTGAATTGCTTTT-3' and

617_R: 5'- AAAAGCAATTCACTGCATCATGCCTGCCACAGCTGGAAGC-3',

631_F: 5'-cy5-TCCCTTTCATTTATTTATCCACAACTTTTAAACATCTGTG-3' and

631_R: 5'-CACAGATGTTTAAAAGTTGTGGATAAATAAATGAAAGGGA-3'

and for the risk alleles (Metabion International AG):

617_F: 5'-cy5-GCTTCCAGCTGTGGCAGGCGTGATGCAGTGAATTGCTTTT-3' and

617_R: 5'-AAAAGCAATTCACTGCATCACGCCTGCCACAGCTGGAAGC- 3',

631_F: 5'-cy5-TCCCTTTCATTTATTTATCTACAACTTTTAAACATCTGTG-3' and

631_R: 5'-CACAGATGTTTAAAAGTTGTAGATAAATAAATGAAAGGGA-3'

The oligonucleotides were annealed and purified from a non-denaturating 12% polyacrylamid gel. 5 μg of nuclear protein extract were incubated with 0.75x EMSA binding buffer (3% glycerol, 0.75 mM MgCl2, 0.375 mM EDTA, 0.375 mM DTT, 37.5 mM NaCl, 7.5 mM TrisHCl pH 7.5) and 90 ng/μl poly-(dIdC) for 10 min on ice, prior to the addition of the labeled oligonucleotide probe. For the competition experiments the cold probe was added in increasing amounts (x11, x33, x66, x100 nM) together with the labeled probe. After adding the oligonucleotide probe the reaction was incubated for additional 20 min on ice and dark. DNA-protein complexes were resolved by electrophoresis for 4 hours on a 5.3% native polyacrylamide gel in 0.5% TBE buffer, at 4 C and dark. The fluorescence of the cy5-labelled oligonucleotides was detected with the Typhoon Trio+ imager (GE Healthcare). The images were processed with the ImageJ and Adobe Photoshop software.

For the supershift assays 1 μg of the rabbit antibody against Ybx1 (Sigma, HPA040304) or control antibody (immunoglobulin from the same species and isotype, santa cruz) was added to the reaction before adding the oligonucleotide probe and was incubated for 30 min on ice. Different conditions such as adding the antibody after the incubation with the oligonucleotide probe, adding in the 0.75x EMSA binding buffer additional 0.625 mM DTT or 0.1 μg/ μl BSA were also examined. All the experiments were repeated at least three times to ensure reproducibility. The analyzed antibodies for Creb1 were: AB3006 (Millipore), 06-519 (Millipore), 9197 (Cell Signaling), 9198 (Cell Signaling) and for Otx3/Dmbx1 were: HPA026811 (Sigma) and sc-47911 (Santa Cruz Biotechnology).

4.7 Affinity chromatography (pull down assay)

For the 617 oligomer, 0.5 mg of nuclear protein extracts from forebrain of E12.5 mouse embryos were incubated with 650 ng of double-stranded biotinylated oligonucleotide probes. Accordingly, for the 631 oligomer I used 2 mg of 393T nuclear extracts and 650 ng double-stranded biotin labeled oligonucleotide probes. The incubation took place in 1x EMSA binding buffer with 0.05 M NaCl, 0.01% CHAPS and Dynabeads® M-280 Streptavidin (Life Technologies) for each allele, 20 min at 4 °C rotating. The sequence of the double-stranded biotin-labeled oligomers used for these experiments is the same with the one used for EMSA, by replacing the *cy5*- with *biotin*-labeling. Incubation with 50 ng/ul (poly-dIdC) succeeded for further 10 min and then three wash steps followed with wash buffer (1x EMSA binding buffer with 0.05 M NaCl). At the end, the proteins were eluted with an ascending salt concentration (200-1250 mM NaCl) of elution buffer (0.83x EMSA binding buffer without salt) and all elutions were examined with EMSA to verify the differential protein elution comparing the two alleles. The affinity chromatography was performed three times. At the end, the elution fractions that showed a difference between the protective and risk allele, were sent for mass spectrometry analysis.

4.8 Mass spectrometry

(in collaboration with Dr. Stefanie Hauck, Research Unit Protein Science, Helmholtz Zentrum München, German Research Center for Environmental Health (GmbH), Neuherberg, Germany)

In solution digestions

Prior to digestion, proteins were precipitated using methanol-chloroform and resuspended in 20 µl of 50 mM ammonium-bicarbonate (ABC) containing Rapigest

(Waters) in a final concentration of 0.2%. Samples were reduced by addition of dithiothreitol (DTT) to a final concentration of 100 mM at 60 °C for 15 min. Cysteines were then alkylated with iodacetamide (Merck) at a final concentration of 300 mM for 30 min at room temperature in the dark. Samples were digested using 1 µg trypsin (Sigma) in 1x TBS at 37 °C overnight (O/N). After digestion, samples were acidified to precipitate and remove Rapigest through centrifugation. Samples were stored at -20 °C until further use.

Mass spectrometry

LC-MS/MS analysis was performed with an HPLC system which is directly coupled to an LTQ Orbitrap XL, as described previously (Merl et al., 2012). A 170 min LC gradient from 5 to 31% of buffer B (98% acetonitrile) at 300 nl/min flow rate has been used, followed by a short gradient from 31 to 95% buffer B in 5 min. From the mass spectrometry prescans, the 10 most abundant peptide ions with at least 200 counts and at least doubly charged were selected for fragmentation. During fragment analysis a high-resolution (60,000 full-width half maximum) mass spectrometry spectrum was acquired in the Orbitrap with a mass range from 200 to 1500 Da. The lock mass option was activated and every ion selected for fragmentation was excluded for 30 sec by dynamic exclusion.

Label-free analysis using Progenesis LC-MS

The acquired spectra were loaded into the Progenesis LC-MS software (version 4.0, Nonlinear) for label free quantification based on peak intensities and analyzed as described previously (Hauck et al., 2010). Briefly, the profile data of the mass spectrometry scans and MS/MS spectra were imported and transformed to peak lists.

The retention times of all samples were aligned to one selected reference sample to create maximal overlay of the two-dimensional feature maps. Features with one charge or ≥8 charges were masked and excluded from further analyses. All remaining features were used to calculate a normalization factor for each sample which corrects for experimental variation. For peptide identification, Mascot (Matrix Science, version 2.3) was set up to search with one missed cleavage allowed, a parent ion tolerance of 10 ppm and a fragment ion mass tolerance of 0.6 Da. Carbamidomethylation was set as fixed modification, methionine oxidation and asparagine or glutamine deamidation were allowed as variable modifications. Spectra were searched against the Ensembl mouse/human database (Release 62; 54576 sequences/ Release°66, 96556 sequences) and a Mascot-integrated decoy database search calculated an average peptide false discovery rate of <2%, when searches were performed with an ion score cutoff of 30 and a significance threshold of $p<0.05$. Peptide assignments were re-imported into Progenesis LC-MS. Normalized abundances of all unique peptides were summed up and allocated to the respective protein. Normalized abundances of the experimental groups were averaged within the groups and fold changes were calculated, comparing the protective (NR) with the risk (R) condition.

4.9 Immunohistochemistry

Mouse embryos were immersion-fixed in 4% paraformaldehyde/PBS and embedded in paraffin. The paraffin sections (8 µm) were deparaffinised in xylene, rehydrated through a graded series of alcohol and ddH_2O. Tissue antigens were retrieved using the heat-induced epitope retrieval (HIER) method. The sections were incubated in 0,01 M NaCitrate buffer (pH 6.0) for 15 min in a microwave oven followed by cooling at room

temperature. To reduce non-specific binding the sections were then incubated for one hour in humid chamber with blocking solution [(no fat milk 5%, 100 mg/ml BSA-Sigma, 100 mg/ml FBS-Gibco) 1:6 diluted in ddH_20] and subsequently with the primary antibody, O/N at 4°C. The next day the sections were washed with PBS and incubated for 75 min at room temperature and light protected with the secondary antibody.

The primary antibodies used were the polyclonal mouse anti-MEIS1 antibody (Abnova, 1:250 dilution), the rabbit anti-YBX1 (Sigma, 1:1:200 dilution), the rabbit anti-phospho-CREB (Ser133) (Millipore, 1:200 dilution), the rabbit anti-DMBX1 (Sigma, 1:50 dilution). The secondary antibodies used were the donkey anti-mouse IgG Alexa Fluor 594 and anti-rabbit IgG Alexa Fluor 488 (Invitrogen, 1:500 dilution). The specificity of the immunoreactions was verified by omission of the primary antibody and by pre-absorption of the antibody with an excess of Meis1 peptide (Abnova, 1:100 dilution).

4.10 *In situ* hybridization (radioactive)

(in collaboration with Dr. Florian Giesert, Institute of Developmental Genetics, Helmholtz Zentrum München, German Research Center for Environmental Health (GmbH), Neuherberg, Germany)

Radioactive in situ hybridization was performed on 8 μm paraffin sections according to a modified published protocol (Dagerlind et al., 1992; Wilkinson et al., 1993). As templates for *in-vitro* transcription of riboprobes, cDNA fragments were used amplified by following primers:

5'-tgtagtttgacgcggtgtgt-3' and 5'-cttgagggcagaagtggaag-3', 5'-ggagcttgtaccaccggtaa-3' and 5'-ccattctccaccgtaacagg-3', 5'-tgtagtttgacgcggtgtg-3' and 5'-gaatggtagtacccggctga-

3', 5'-ggcctgcagacattaaccat-3' and 5'-cttgagggcagaagtggaag-3', 5'-actccagcgagatccggg-3' and 5'-gcaaaagcagaaatgaatgaa-3' (Lin et al., 2010) for Creb1;

5'-tcaggtggtgagatggacaa-3' and 5'-gtcagagggcaaaaagcaag-3' for Ybx1.

As a general note, RNase free solutions and materials were used to avoid degradation of the mRNA and the RNA probe.

Synthesis of ^{35}S labelled RNA probes

Radioactively labelled RNA probes were generated by *in-vitro* transcription with an appropriate RNA polymerase (T7 and SP6) in the presence of [α-thio^{35}S]-UTP. As templates, pCRII-TOPO plasmids (Invitrogen) containing part/ or the whole cDNA of the gene to examine were linearized with an appropriate restriction enzyme cutting downstream of the end of the cDNA sequence. The 1x transcription reaction was as follows:

Amount	Reagent
3 µl	10x transcription buffer
3 µl	dNTP mix (rATP/rCTP/rGTP 10mM each)
1 µl	0.5 M DTT
1 µl	RNasin (RNase inhibitor; 40U/µl)
1.5 µg	linearised plasmid DNA template
7 µl	[α-thio-^{35}S]-UTP (12.5 mCi/mM)
x µl	H_2O (total volume is 30µl)
1 µl	RNA polymerase (T7 or SP6; 20U/µl)

30 µl total volume

The reaction was incubated at 37 °C for 3 hours. Afterwards, the DNA template was digested with 2 µl of RNase-free DNase I, at 37 °C for 15 min. Probes were purified with the RNeasy Mini Kit following manufacturer's instructions and activity was measured with a liquid scintillation counter.

Hybridization

The hybridization temperature was assigned approximately 25 °C below the melting temperature of the probe. Before hybridization paraffin sections were dewaxed and treated as follows:

Day 1

Incubation t [min]	Reagent
2 x 15	Rotihistol
2 x 5	100% ethanol
5	70% ethanol
3	DEPC-H20
3	PBS/DEPC
20	4% PFA/PBS
2 x 5	PBS/DEPC
7	20 µg/ml proteinase K in proteinase-K-buffer
5	PBS/DEPC
20	4% PFA/PBS
5	PBS/DEPC
10	200 ml of rapidly stirring 0.1 M triethanolamine-HCl (pH 8.0) (TEA)

Slides were air dried and used immediately for prehybridization, by incubation with Hyb-mix (without labelled riboprobe) for 1hour at hybridization temperature. For hybridization the protocol below was followed:

1. Prepare appropriate amount of hybridisation mix containing 35000 to 70000 cpm/µl
2. Heat hybridisation mix containing the probe to 90 °C for 2 min
3. Incubate shortly on ice, then on RT

4. After prehybridization remove coverslip and as much liquid as possible. Immediately proceed with hybridisation

5. Apply 90 to 100µl of hybridization mix containing 35000 to 70000 cpm/µl per slide on the slide and cover carefully with coverslip

6. Place slides carefully into a hybridization chamber containing hybridization chamber fluid to avoid drying out of the hybridization mix

7. Incubate in an oven at 55-68 °C O/N (up to 20 hours)

Day 2

Incubation t [min]	Incubation T [°C]	Reagent
4 x 5	RT	4x SSC (saline-sodium citrate buffer)
20	37	NTE (20 µg/ml RNase A)
2 x 5	RT	2x SSC/1 mM DTT
10	RT	1x SSC/1 mM DTT
10	RT	0.5x SSC/1mM DTT
2 x 30	64	0.1x SSC/1 mM DTT
2 x 10	RT	0.1x SSC
1	RT	30% ethanol in 300 mM NH_4OAc
1	RT	50% ethanol in 300 mM NH_4OAc
1	RT	70% ethanol in 300 mM NH_4OAc
1	RT	95% ethanol
2 x 1	RT	100% ethanol

Slides were air dried and exposed to an autoradiography film (BioMax MR) for 2 days. For further analysis slides were dipped in a photo emulsion (diluted 1:1 with water) and stored at 4 °C in dark for an appropriate time depending on the signal intensity (estimated by the results from the autoradiography film). Finally, slides were equilibrated for 1 hour at RT, developed for 5 min, rinsed with water and fixed for 7 min. After rinsing the slides for 25 min in floating tap water, the remaining emulsion was removed and slides were counterstained with cresyl violet.

Nissl staining (cresyl violet)

Nissl staining of paraffin sections was performed according to the following scheme:

Incubation t	Step: Reagent
1 - 5 min	staining: cresyl violet staining solution
	rinse: H_2O
1 min	clearing: 70% ethanol until slide is clear
10 - 60 sec	clearing: 96% ethanol + 0.5% acetic acid
2 x 1 min	dehydration: 96% ethanol
2 x 2 min	dehydration: 100% ethanol
2 x 10 min	xylol

Slides were covered immediately with DPX and dried O/N under the hood.

4.11 Imaging

All histological slides were imaged using the following microscopes: Zeiss Axioplan2 upright light/fluorescence Microscope (objective 5x–100x) and the binocular microscope: Zeiss, Stemi SV 6 (planobjective S 1.0x). Images were taken using the digital camera AxioCam MRC with the Axiovision 4.6 software. Images were edited, if necessary, using the program Adobe-Photoshop® (version 7.0), by changing contrast and brightness. Anatomical structures were identified and termed according to the histological atlas “Atlas of the prenatal mouse brain” (Schambra, 1992).

4.12 Buffers and solutions

Most of the buffers and solutions used are described in the method parts that belong to. In this section only solutions that are not included in the previous sections are mentioned.

Solutions for *in situ* hybridisation (radioactive and non-radioactive)	**Composition**
chamber fluid	50% formamide 2x SSC
hybridisation mix	50% formamide 20 mM Tris-HCl, pH 8.0 300 mM NaCl 5 mM EDTA, pH8.0 10% dextran sulfate 0.02% Ficoll-400 0.02% PVP-40 0.02% BSA 0.5 mg/ml tRNA 0.2 mg/ml carrier DNA 20 mM DTT
NTE buffer (5x)	0.5 M NaCl 10 mM Tris-HCl, pH 8.0 5 mM EDTA, pH 8.0
proteinase K buffer	50 mM Tris-HCl, pH 7.6 5 mM EDTA pH 8.0
triethanolamine solution	0.1 M triethanolamine adjust to pH 8.0
ammonium acetate stock solution (10x)	3 M NH_4OAc
PK buffer (2x)	100 mM Tris 10 mM EDTA pH 8.0

PBT	1x PBS 0.05% Tween-20
NTE (5x)	2.5 M NaCl 50 mM Tris 8.0 25 mM EDTA
TN (10x)	1 M Tris 1.5 M NaCl Solve TN 1hour at 60 °C
TNT	1x TN 0.05% Tween-20
TNB	1x TN 0.5% blocking reagent (NEN)
TMN (or MTN)	0,1 M Tris 0,1 M NaCl 0,05 M $MgCl_2$-$6H_2O$
Maleat buffer	150 mM NaCl 100 mM maleic acid adjust to pH 7.5
cresylviolet staining solution (Nissl)	0.5% cresylviolet 2.5 mM sodium acetate 0.31% acetic acid ad 500 ml H_2O filter before use

EMSA Gel (5,3%) [Volume]	**Composition**
25 ml	1x TBE
15 ml	37,5:1 acrylamide/bisacrylamide (40%w/v)

1562,5µl	80%v/v Glycerol
7 ml	ddH_2O
375 µl	10% APS
25 µl	TEMED

5x TBE	**Composition**
54 gr	Tris Base
27.5 gr	Boric acid
20ml	0.5M EDTA pH 8,0
Up to 1 Liter	ddH_2O, final pH 8.3

5 ETHICS

The protocols for subject recruitment and assessment and the informed consent for participants were reviewed and approved by the local ethical committee (Bayerische Landesärztekammer).

All animal work was performed in accordance with the German Animal Welfare Act and the Spanish Ethical Committee for Animal Research from Consejo Superior de Investigaciones (CSIC).

6 ACKNOWLEDGMENTS

I would like to thank my supervisor, Prof. Juliane Winkelmann, who believed in me and supported me to carry on till the end. Thank you to my other two supervisors, Prof. Hemmer and Prof. Meitinger, especially the last one, for his constant judgment and trigger that pushed me forward all the time. Thanks to my Prof. in Greece, Georgios Hadjigeorgiou for inspiring me at the first place.

A big thank you to all my colleagues (Derek Spieler, Barbara Schormair, Franziska Knauf, Eva Schulte) that spent four whole years with me in the laboratory with many ups and downs. Thank you Jelena Golic, Carola Fischer, Jenifer Behler for your technical support. Thank you Matteo Gorza for “baptizing” me in the world of proteomics. A special thanks to my dear Irmgard Zaus also for her technical support and just for being there and listening to me.

I would like to thank all of the people and collaborators that helped me throughout my project. Thank you Dr. Katrin Offe and Desislava Zlatanova for supporting me these four years of my PhD. I thank Mr. Johannes Tritschler for his support in mathematics-statistics and Dr. Jürgen Zschocke for his time to discuss scientifically and his help. A special thanks to Dr. Miguel Torres, Daniel Mateos San Martin and my dear Laura Carramolino for their warm hospitality in Madrid and the high-level of scientific feedback. I would like to thank Dr. Helmut Laumen for his cooperation and all the members of his group (Manu, Lisssy, Kun) that accepted me with wide open arms. Special thanks to my close colleague and dear friend the last year Heekyoung Lee! Your smile and supportive words made me feel good all the time! At last, I would like to thank Dr. Stefanie Hauck

and Dr. Christine von Törne for their cooperation, support and helpful feedback during the mass spectrometry analysis.

Thank you Anna, Georgia, Maria, Kallia, Fotini for being part of my life and friends that last forever. Thank you Adeline, Cathy, Arcangela, Marijana for also being good friends!

The last words are kept for the most special people in my life. A special thanks to my aunt Vassiliki, uncle Giannis and cousins Maria and Dimis, for letting me be part of the family here in Munich. I would like to express my deep love and gratitude for everything to my parents, Nelli (Garyfallia) and Giorgos, and my brother Nassos. Thank you for your love and support through this big journey of ten years studying. I hope I make you proud and wish to be closer to you again. I would like to express also my love to my grandparents, Eleni and Athanasios - Maria and Dimitris, for their care and support. At the end, I want to express my deep love and gratitude to my life's companion Tobias, who I indeed met via this PhD program. Your support and love will be my inner strength that mobilizes me in the journey through life.

At last, I express my gratitude to God. Without His support nothing from all of these could happen...

7 REFERENCES

Allen Brain Atlas [database on the Internet]. Allen Institute for Brain Science. 2012 Available from: http://www.brain-map.org.

Allen RP, Barker PB, Wehrl F, Song HK, Earley CJ. MRI measurement of brain iron in patients with restless legs syndrome. Neurology. 2001 Jan 23;56(2):263-5.

Allen RP, Earley CJ. Defining the phenotype of the restless legs syndrome (RLS) using age-of-symptom-onset. Sleep Med. 2000 Feb 1;1(1):11-9.

Allen RP, Kushida CA, Atkinson MJ. Factor analysis of the International Restless Legs Syndrome Study Group's scale for restless legs severity. Sleep Med. 2003a Mar;4(2):133-5.

Allen RP, La Buda MC, Becker P, Earley CJ. Family history study of the restless legs syndrome. Sleep Med. 2002 Nov;3 Suppl:S3-7.

Allen RP, Picchietti D, Hening WA, Trenkwalder C, Walters AS, Montplaisi J. Restless legs syndrome: diagnostic criteria, special considerations, and epidemiology. A report from the restless legs syndrome diagnosis and epidemiology workshop at the National Institutes of Health. Sleep Med. 2003b Mar;4(2):101-19.

Allende ML, Manzanares M, Tena JJ, Feijoo CG, Gomez-Skarmeta JL. Cracking the genome's second code: enhancer detection by combined phylogenetic footprinting and transgenic fish and frog embryos. Methods. 2006 Jul;39(3):212-9.

Ancoli-Israel S, Seifert AR, Lemon M. Thermal biofeedback and periodic movements in sleep: patients' subjective reports and a case study. Biofeedback Self Regul. 1986 Sep;11(3):177-88.

Astrakas LG, Konitsiotis S, Margariti P, Tsouli S, Tzarouhi L, Argyropoulou MI. T2 relaxometry and fMRI of the brain in late-onset restless legs syndrome. Neurology. 2008 Sep 16;71(12):911-6.

Azcoitia V, Aracil M, Martinez AC, Torres M. The homeodomain protein Meis1 is essential for definitive hematopoiesis and vascular patterning in the mouse embryo. Dev Biol. 2005 Apr 15;280(2):307-20.

Bader AG, Vogt PK. Inhibition of protein synthesis by Y box-binding protein 1 blocks oncogenic cell transformation. Mol Cell Biol. 2005 Mar;25(6):2095-106.

Bara-Jimenez W, Aksu M, Graham B, Sato S, Hallett M. Periodic limb movements in sleep: state-dependent excitability of the spinal flexor reflex. Neurology. 2000 Apr 25;54(8):1609-16.

Barco A, Marie H. Genetic approaches to investigate the role of CREB in neuronal plasticity and memory. Mol Neurobiol. 2011 Dec;44(3):330-49.

Bardwell VJ, Treisman R. The POZ domain: a conserved protein-protein interaction motif. Genes Dev. 1994 Jul 15;8(14):1664-77.

Bargou RC, Jurchott K, Wagener C, Bergmann S, Metzner S, Bommert K, et al. Nuclear localization and increased levels of transcription factor YB-1 in primary human breast cancers are associated with intrinsic MDR1 gene expression. Nat Med. 1997 Apr;3(4):447-50.

Bassetti CL, Mauerhofer D, Gugger M, Mathis J, Hess CW. Restless legs syndrome: a clinical study of 55 patients. Eur Neurol. 2001;45(2):67-74.

Bendotti C, Bao Cutrona M, Cheroni C, Grignaschi G, Lo Coco D, Peviani M, et al. Inter- and intracellular signaling in amyotrophic lateral sclerosis: role of p38 mitogen-activated protein kinase. Neurodegener Dis. 2005;2(3-4):128-34.

Benes H, von Eye A, Kohnen R. Empirical evaluation of the accuracy of diagnostic criteria for Restless Legs Syndrome. Sleep Med. 2009 May;10(5):524-30.

Berger K, Luedemann J, Trenkwalder C, John U, Kessler C. Sex and the risk of restless legs syndrome in the general population. Arch Intern Med. 2004 Jan 26;164(2):196-202.

Berkowitz LA, Gilman MZ. Two distinct forms of active transcription factor CREB (cAMP response element binding protein). Proc Natl Acad Sci U S A. 1990 Jul;87(14):5258-62.

Berriz GF, King OD, Bryant B, Sander C, Roth FP. Characterizing gene sets with FuncAssociate. Bioinformatics. 2003 Dec 12;19(18):2502-4.

Bonati MT, Ferini-Strambi L, Aridon P, Oldani A, Zucconi M, Casari G. Autosomal dominant restless legs syndrome maps on chromosome 14q. Brain. 2003 Jun;126(Pt 6):1485-92.

Braun RE. Temporal control of protein synthesis during spermatogenesis. Int J Androl. 2000;23 Suppl 2:92-4.

Bucher SF, Trenkwalder C, Oertel WH. Reflex studies and MRI in the restless legs syndrome. Acta Neurol Scand. 1996 Aug;94(2):145-50.

Carlezon WA, Jr., Duman RS, Nestler EJ. The many faces of CREB. Trends Neurosci. 2005 Aug;28(8):436-45.

Cartharius K, Frech K, Grote K, Klocke B, Haltmeier M, Klingenhoff A, et al. MatInspector and beyond: promoter analysis based on transcription factor binding sites. Bioinformatics. 2005 Jul 1;21(13):2933-42.

Cavanaugh JE, Jaumotte JD, Lakoski JM, Zigmond MJ. Neuroprotective role of ERK1/2 and ERK5 in a dopaminergic cell line under basal conditions and in response to oxidative stress. J Neurosci Res. 2006 Nov 1;84(6):1367-75.

Celle S, Roche F, Peyron R, Faillenot I, Laurent B, Pichot V, et al. Lack of specific gray matter alterations in restless legs syndrome in elderly subjects. J Neurol. 2010 Mar;257(3):344-8.

Cervenka S, Palhagen SE, Comley RA, Panagiotidis G, Cselenyi Z, Matthews JC, et al. Support for dopaminergic hypoactivity in restless legs syndrome: a PET study on D2-receptor binding. Brain. 2006 Aug;129(Pt 8):2017-28.

Chen S, Ondo WG, Rao S, Li L, Chen Q, Wang Q. Genomewide linkage scan identifies a novel susceptibility locus for restless legs syndrome on chromosome 9p. Am J Hum Genet. 2004 May;74(5):876-85.

Coleman RM, Bliwise DL, Sajben N, Boomkamp A, de Bruyn LM, Dement WC. Daytime sleepiness in patients with periodic movements in sleep. Sleep. 1982;5 Suppl 2:S191-202.

Connor JR, Boyer PJ, Menzies SL, Dellinger B, Allen RP, Ondo WG, et al. Neuropathological examination suggests impaired brain iron acquisition in restless legs syndrome. Neurology. 2003 Aug 12;61(3):304-9.

Connor JR, Wang XS, Allen RP, Beard JL, Wiesinger JA, Felt BT, et al. Altered dopaminergic profile in the putamen and substantia nigra in restless leg syndrome. Brain. 2009 Sep;132(Pt 9):2403-12.

Connor JR, Wang XS, Patton SM, Menzies SL, Troncoso JC, Earley CJ, et al. Decreased transferrin receptor expression by neuromelanin cells in restless legs syndrome. Neurology. 2004 May 11;62(9):1563-7.

Dagerlind A, Friberg K, Bean AJ, Hokfelt T. Sensitive mRNA detection using unfixed tissue: combined radioactive and non-radioactive in situ hybridization histochemistry. Histochemistry. 1992 Aug;98(1):39-49.

Dasen JS, Tice BC, Brenner-Morton S, Jessell TM. A Hox regulatory network establishes motor neuron pool identity and target-muscle connectivity. Cell. 2005 Nov 4;123(3):477-91.

DeAndrade MP, Johnson RL, Jr., Unger EL, Zhang L, van Groen T, Gamble KL, et al. Motor restlessness, sleep disturbances, thermal sensory alterations and elevated serum iron levels in Btbd9 mutant mice. Hum Mol Genet. 2012 Sep 15;21(18):3984-92.

Desai AV, Cherkas LF, Spector TD, Williams AJ. Genetic influences in self-reported symptoms of obstructive sleep apnoea and restless legs: a twin study. Twin Res. 2004 Dec;7(6):589-95.

Desautels A, Turecki G, Montplaisir J, Sequeira A, Verner A, Rouleau GA. Identification of a major susceptibility locus for restless legs syndrome on chromosome 12q. Am J Hum Genet. 2001 Dec;69(6):1266-70.

Desautels A, Turecki G, Montplaisir J, Xiong L, Walters AS, Ehrenberg BL, et al. Restless legs syndrome: confirmation of linkage to chromosome 12q, genetic heterogeneity, and evidence of complexity. Arch Neurol. 2005 Apr;62(4):591-6.

Dhillon AS, Hagan S, Rath O, Kolch W. MAP kinase signalling pathways in cancer. Oncogene. 2007 May 14;26(22):3279-90.

Dinev D, Jordan BW, Neufeld B, Lee JD, Lindemann D, Rapp UR, et al. Extracellular signal regulated kinase 5 (ERK5) is required for the differentiation of muscle cells. EMBO Rep. 2001 Sep;2(9):829-34.

Dubchak I, Brudno M, Loots GG, Pachter L, Mayor C, Rubin EM, et al. Active conservation of noncoding sequences revealed by three-way species comparisons. Genome Res. 2000 Sep;10(9):1304-6.

Earley CJ, Allen RP, Beard JL, Connor JR. Insight into the pathophysiology of restless legs syndrome. J Neurosci Res. 2000 Dec 1;62(5):623-8.

Earley CJ, Allen RP, Connor JR, Ferrucci L, Troncoso J. The dopaminergic neurons of the A11 system in RLS autopsy brains appear normal. Sleep Med. 2009 Dec;10(10):1155-7.

Earley CJ, Connor JR, Beard JL, Clardy SL, Allen RP. Ferritin levels in the cerebrospinal fluid and restless legs syndrome: effects of different clinical phenotypes. Sleep. 2005 Sep;28(9):1069-75.

Earley CJ, Connor JR, Beard JL, Malecki EA, Epstein DK, Allen RP. Abnormalities in CSF concentrations of ferritin and transferrin in restless legs syndrome. Neurology. 2000 Apr 25;54(8):1698-700.

Earley CJ, Kuwabara H, Wong DF, Gamaldo C, Salas R, Brasic J, et al. The dopamine transporter is decreased in the striatum of subjects with restless legs syndrome. Sleep. 2011 Mar;34(3):341-7.

Easton DF, Pooley KA, Dunning AM, Pharoah PD, Thompson D, Ballinger DG, et al. Genome-wide association study identifies novel breast cancer susceptibility loci. Nature. 2007 Jun 28;447(7148):1087-93.

Eisensehr I, Wetter TC, Linke R, Noachtar S, von Lindeiner H, Gildehaus FJ, et al. Normal IPT and IBZM SPECT in drug-naive and levodopa-treated idiopathic restless legs syndrome. Neurology. 2001 Oct 9;57(7):1307-9.

Ekbom KA. Restless legs syndrome. Neurology. 1960 Sep;10:868-73.

El-Amraoui A, Petit C. Cadherins as targets for genetic diseases. Cold Spring Harb Perspect Biol. 2010 Jan;2(1):a003095.

Erickson T, French CR, Waskiewicz AJ. Meis1 specifies positional information in the retina and tectum to organize the zebrafish visual system. Neural Dev. 2010;5:22.

Esparza SD, Chang J, Shankar DB, Zhang B, Nelson SF, Sakamoto KM. CREB regulates Meis1 expression in normal and malignant hematopoietic cells. Leukemia. 2008 Mar;22(3):665-7.

Evdokimova V, Ruzanov P, Imataka H, Raught B, Svitkin Y, Ovchinnikov LP, et al. The major mRNA-associated protein YB-1 is a potent 5' cap-dependent mRNA stabilizer. Embo J. 2001 Oct 1;20(19):5491-502.

Faustino NA, Cooper TA. Pre-mRNA splicing and human disease. Genes Dev. 2003 Feb 15;17(4):419-37.

Freeman A, Pranski E, Miller RD, Radmard S, Bernhard D, Jinnah HA, et al. Sleep fragmentation and motor restlessness in a Drosophila model of Restless Legs Syndrome. Curr Biol. 2012 Jun 19;22(12):1142-8.

Frye BC, Halfter S, Djudjaj S, Muehlenberg P, Weber S, Raffetseder U, et al. Y-box protein-1 is actively secreted through a non-classical pathway and acts as an extracellular mitogen. EMBO Rep. 2009 Jul;10(7):783-9.

Fujimoto W, Shiuchi T, Miki T, Minokoshi Y, Takahashi Y, Takeuchi A, et al. Dmbx1 is essential in agouti-related protein action. Proc Natl Acad Sci U S A. 2007 Sep 25;104(39):15514-9.

Garcia-Borreguero D, Larrosa O, de la Llave Y, Verger K, Masramon X, Hernandez G. Treatment of restless legs syndrome with gabapentin: a double-blind, cross-over study. Neurology. 2002 Nov 26;59(10):1573-9.

Godau J, Klose U, Di Santo A, Schweitzer K, Berg D. Multiregional brain iron deficiency in restless legs syndrome. Mov Disord. 2008 Jun 15;23(8):1184-7.

Godau J, Schweitzer KJ, Liepelt I, Gerloff C, Berg D. Substantia nigra hypoechogenicity: definition and findings in restless legs syndrome. Mov Disord. 2007 Jan 15;22(2):187-92.

Godt D, Couderc JL, Cramton SE, Laski FA. Pattern formation in the limbs of Drosophila: bric a brac is expressed in both a gradient and a wave-like pattern and is required for specification and proper segmentation of the tarsus. Development. 1993 Nov;119(3):799-812.

Gross MK, Dottori M, Goulding M. Lbx1 specifies somatosensory association interneurons in the dorsal spinal cord. Neuron. 2002 May 16;34(4):535-49.

Hanson M, Honour M, Singleton A, Crawley A, Hardy J, Gwinn-Hardy K. Analysis of familial and sporadic restless legs syndrome in age of onset, gender, and severity features. J Neurol. 2004 Nov;251(11):1398-401.

Hauck SM, Dietter J, Kramer RL, Hofmaier F, Zipplies JK, Amann B, et al. Deciphering membrane-associated molecular processes in target tissue of autoimmune uveitis by label-free quantitative mass spectrometry. Mol Cell Proteomics. 2010 Oct;9(10):2292-305.

Hening WA. Restless legs syndrome: the most common and least diagnosed sleep disorder. Sleep Med. 2004 Sep;5(5):429-30.

Hipfel R, Schittek B, Bodingbauer Y, Garbe C. Specifically regulated genes in malignant melanoma tissues identified by subtractive hybridization. Br J Cancer. 2000 Mar;82(6):1149-57.

Hogl B, Kiechl S, Willeit J, Saletu M, Frauscher B, Seppi K, et al. Restless legs syndrome: a community-based study of prevalence, severity, and risk factors. Neurology. 2005 Jun 14;64(11):1920-4.

Hornyak M, Ahrendts JC, Spiegelhalder K, Riemann D, Voderholzer U, Feige B, et al. Voxel-based morphometry in unmedicated patients with restless legs syndrome. Sleep Med. 2007 Dec;9(1):22-6.

Hornyak M, Feige B, Voderholzer U, Philipsen A, Riemann D. Polysomnography findings in patients with restless legs syndrome and in healthy controls: a comparative observational study. Sleep. 2007 Jul;30(7):861-5.

Huang H, Rastegar M, Bodner C, Goh SL, Rambaldi I, Featherstone M. MEIS C termini harbor transcriptional activation domains that respond to cell signaling. J Biol Chem. 2005 Mar 18;280(11):10119-27.

Jagasia R, Steib K, Englberger E, Herold S, Faus-Kessler T, Saxe M, et al. GABA-cAMP response element-binding protein signaling regulates maturation and survival of newly generated neurons in the adult hippocampus. J Neurosci. 2009 Jun 24;29(25):7966-77.

Jurchott K, Bergmann S, Stein U, Walther W, Janz M, Manni I, et al. YB-1 as a cell cycle-regulated transcription factor facilitating cyclin A and cyclin B1 gene expression. J Biol Chem. 2003 Jul 25;278(30):27988-96.

Kamura T, Yahata H, Amada S, Ogawa S, Sonoda T, Kobayashi H, et al. Is nuclear expression of Y box-binding protein-1 a new prognostic factor in ovarian serous adenocarcinoma? Cancer. 1999 Jun 1;85(11):2450-4.

Kemlink D, Plazzi G, Vetrugno R, Provini F, Polo O, Stiasny-Kolster K, et al. Suggestive evidence for linkage for restless legs syndrome on chromosome 19p13. Neurogenetics. 2008 May;9(2):75-82.

Kemlink D, Polo O, Montagna P, Provini F, Stiasny-Kolster K, Oertel W, et al. Family-based association study of the restless legs syndrome loci 2 and 3 in a European population. Mov Disord. 2007 Jan 15;22(2):207-12.

Kohno K, Izumi H, Uchiumi T, Ashizuka M, Kuwano M. The pleiotropic functions of the Y-box-binding protein, YB-1. Bioessays. 2003 Jul;25(7):691-8.

Kreusch A, Pfaffinger PJ, Stevens CF, Choe S. Crystal structure of the tetramerization domain of the Shaker potassium channel. Nature. 1998 Apr 30;392(6679):945-8.

Kruger M, Schafer K, Braun T. The homeobox containing gene Lbx1 is required for correct dorsal-ventral patterning of the neural tube. J Neurochem. 2002 Aug;82(4):774-82.

Lavigne GJ, Montplaisir JY. Restless legs syndrome and sleep bruxism: prevalence and association among Canadians. Sleep. 1994 Dec;17(8):739-43.

Lee B, Li A, Hansen KF, Cao R, Yoon JH, Obrietan K. CREB influences timing and entrainment of the SCN circadian clock. J Biol Rhythms. 2010 Dec;25(6):410-20.

Levchenko A, Montplaisir JY, Dube MP, Riviere JB, St-Onge J, Turecki G, et al. The 14q restless legs syndrome locus in the French Canadian population. Ann Neurol. 2004 Jun;55(6):887-91.

Levchenko A, Provost S, Montplaisir JY, Xiong L, St-Onge J, Thibodeau P, et al. A novel autosomal dominant restless legs syndrome locus maps to chromosome 20p13. Neurology. 2006 Sep 12;67(5):900-1.

Liebetanz KM, Winkelmann J, Trenkwalder C, Putz B, Dichgans M, Gasser T, et al. RLS3: fine-mapping of an autosomal dominant locus in a family with intrafamilial heterogeneity. Neurology. 2006 Jul 25;67(2):320-1.

Lin CH, Chen CM, Hou YT, Wu YR, Hsieh-Li HM, Su MT, et al. The CAG repeat in SCA12 functions as a cis element to up-regulate PPP2R2B expression. Hum Genet. 2010 Aug;128(2):205-12.

Linke R, Eisensehr I, Wetter TC, Gildehaus FJ, Popperl G, Trenkwalder C, et al. Presynaptic dopaminergic function in patients with restless legs syndrome: are there common features with early Parkinson's disease? Mov Disord. 2004 Oct;19(10):1158-62.

Lochhead PA, Gilley R, Cook SJ. ERK5 and its role in tumour development. Biochem Soc Trans. 2012 Feb;40(1):251-6.

Lohmann-Hedrich K, Neumann A, Kleensang A, Lohnau T, Muhle H, Djarmati A, et al. Evidence for linkage of restless legs syndrome to chromosome 9p: are there two distinct loci? Neurology. 2008 Feb 26;70(9):686-94.

Maeda R, Mood K, Jones TL, Aruga J, Buchberg AM, Daar IO. Xmeis1, a protooncogene involved in specifying neural crest cell fate in Xenopus embryos. Oncogene. 2001 Mar 15;20(11):1329-42.

Mantamadiotis T, Lemberger T, Bleckmann SC, Kern H, Kretz O, Martin Villalba A, et al. Disruption of CREB function in brain leads to neurodegeneration. Nat Genet. 2002 May;31(1):47-54.

Margariti PN, Astrakas LG, Tsouli SG, Hadjigeorgiou GM, Konitsiotis S, Argyropoulou MI. Investigation of unmedicated early onset restless legs syndrome by voxel-based morphometry, T2 relaxometry, and functional MR imaging during the night-time hours. AJNR Am J Neuroradiol. 2012 Apr;33(4):667-72.

Marques CA, Keil U, Bonert A, Steiner B, Haass C, Muller WE, et al. Neurotoxic mechanisms caused by the Alzheimer's disease-linked Swedish amyloid precursor protein mutation: oxidative stress, caspases, and the JNK pathway. J Biol Chem. 2003 Jul 25;278(30):28294-302.

Mathias RA, Beaty TH, Bailey-Wilson JE, Bickel C, Stockton ML, Barnes KC. Inheritance of total serum IgE in the isolated Tangier Island population from Virginia: complexities associated with genealogical depth of pedigrees in segregation analyses. Hum Hered. 2005;59(4):228-38.

Matsumoto K, Wolffe AP. Gene regulation by Y-box proteins: coupling control of transcription and translation. Trends Cell Biol. 1998 Aug;8(8):318-23.

Matthews RP, Guthrie CR, Wailes LM, Zhao X, Means AR, McKnight GS. Calcium/calmodulin-dependent protein kinase types II and IV differentially regulate CREB-dependent gene expression. Mol Cell Biol. 1994 Sep;14(9):6107-16.

Mercader N, Leonardo E, Azpiazu N, Serrano A, Morata G, Martinez C, et al. Conserved regulation of proximodistal limb axis development by Meis1/Hth. Nature. 1999 Nov 25;402(6760):425-9.

Mercader N, Leonardo E, Piedra ME, Martinez AC, Ros MA, Torres M. Opposing RA and FGF signals control proximodistal vertebrate limb development through regulation of Meis genes. Development. 2000 Sep;127(18):3961-70.

Mercader N, Tanaka EM, Torres M. Proximodistal identity during vertebrate limb regeneration is regulated by Meis homeodomain proteins. Development. 2005 Sep;132(18):4131-42.

Merl J, Ueffing M, Hauck SM, von Toerne C. Direct comparison of MS-based label-free and SILAC quantitative proteome profiling strategies in primary retinal Muller cells. Proteomics. 2012 Jun;12(12):1902-11.

Michaud M, Paquet J, Lavigne G, Desautels A, Montplaisir J. Sleep laboratory diagnosis of restless legs syndrome. Eur Neurol. 2002;48(2):108-13.

Michaud M, Soucy JP, Chabli A, Lavigne G, Montplaisir J. SPECT imaging of striatal pre- and postsynaptic dopaminergic status in restless legs syndrome with periodic leg movements in sleep. J Neurol. 2002 Feb;249(2):164-70.

Mizuhara E, Nakatani T, Minaki Y, Sakamoto Y, Ono Y. Corl1, a novel neuronal lineage-specific transcriptional corepressor for the homeodomain transcription factor Lbx1. J Biol Chem. 2005 Feb 4;280(5):3645-55.

Mizuno S, Mihara T, Miyaoka T, Inagaki T, Horiguchi J. CSF iron, ferritin and transferrin levels in restless legs syndrome. J Sleep Res. 2005 Mar;14(1):43-7.

Montplaisir J, Boucher S, Poirier G, Lavigne G, Lapierre O, Lesperance P. Clinical, polysomnographic, and genetic characteristics of restless legs syndrome: a study of 133 patients diagnosed with new standard criteria. Mov Disord. 1997 Jan;12(1):61-5.

Nair P, De Preter K, Vandesompele J, Speleman F, Stallings RL. Aberrant splicing of the PTPRD gene mimics microdeletions identified at this locus in neuroblastomas. Genes Chromosomes Cancer. 2008 Mar;47(3):197-202.

Numoto M, Niwa O, Kaplan J, Wong KK, Merrell K, Kamiya K, et al. Transcriptional repressor ZF5 identifies a new conserved domain in zinc finger proteins. Nucleic Acids Res. 1993 Aug 11;21(16):3767-75.

Oda Y, Sakamoto A, Shinohara N, Ohga T, Uchiumi T, Kohno K, et al. Nuclear expression of YB-1 protein correlates with P-glycoprotein expression in human osteosarcoma. Clin Cancer Res. 1998 Sep;4(9):2273-7.

Ohtoshi A, Behringer RR. Neonatal lethality, dwarfism, and abnormal brain development in Dmbx1 mutant mice. Mol Cell Biol. 2004 Sep;24(17):7548-58.

Ohtoshi A, Nishijima I, Justice MJ, Behringer RR. Dmbx1, a novel evolutionarily conserved paired-like homeobox gene expressed in the brain of mouse embryos. Mech Dev. 2002 Jan;110(1-2):241-4.

Ondo W, Jankovic J. Restless legs syndrome: clinicoetiologic correlates. Neurology. 1996 Dec;47(6):1435-41.

Ondo WG, Vuong KD, Wang Q. Restless legs syndrome in monozygotic twins: clinical correlates. Neurology. 2000 Nov 14;55(9):1404-6.

Oppenheim H, editor. Lehrbuch der nervenkrankheiten. Berlin: S. Karger; 1923.

Perissi V, Aggarwal A, Glass CK, Rose DW, Rosenfeld MG. A corepressor/coactivator exchange complex required for transcriptional activation by nuclear receptors and other regulated transcription factors. Cell. 2004 Feb 20;116(4):511-26.

Pfeufer A, van Noord C, Marciante KD, Arking DE, Larson MG, Smith AV, et al. Genome-wide association study of PR interval. Nat Genet. 2010 Feb;42(2):153-9.

Phillips B, Hening W, Britz P, Mannino D. Prevalence and correlates of restless legs syndrome: results from the 2005 National Sleep Foundation Poll. Chest. 2006 Jan;129(1):76-80.

Phillips B, Young T, Finn L, Asher K, Hening WA, Purvis C. Epidemiology of restless legs symptoms in adults. Arch Intern Med. 2000 Jul 24;160(14):2137-41.

Pichler I, Marroni F, Volpato CB, Gusella JF, Klein C, Casari G, et al. Linkage analysis identifies a novel locus for restless legs syndrome on chromosome 2q in a South Tyrolean population isolate. Am J Hum Genet. 2006 Oct;79(4):716-23.

Pruunsild P, Sepp M, Orav E, Koppel I, Timmusk T. Identification of cis-elements and transcription factors regulating neuronal activity-dependent transcription of human BDNF gene. J Neurosci. 2011 Mar 2;31(9):3295-308.

Qu S, Le W, Zhang X, Xie W, Zhang A, Ondo WG. Locomotion is increased in a11-lesioned mice with iron deprivation: a possible animal model for restless legs syndrome. J Neuropathol Exp Neurol. 2007 May;66(5):383-8.

Raffetseder U, Frye B, Rauen T, Jurchott K, Royer HD, Jansen PL, et al. Splicing factor SRp30c interaction with Y-box protein-1 confers nuclear YB-1 shuttling and alternative splice site selection. J Biol Chem. 2003 May 16;278(20):18241-8.

Ramsey AJ, Hillas PJ, Fitzpatrick PF. Characterization of the active site iron in tyrosine hydroxylase. Redox states of the iron. J Biol Chem. 1996 Oct 4;271(40):24395-400.

Rijsman RM, Stam CJ, de Weerd AW. Abnormal H-reflexes in periodic limb movement disorder; impact on understanding the pathophysiology of the disorder. Clin Neurophysiol. 2005 Jan;116(1):204-10.

Riviere JB, Xiong L, Levchenko A, St-Onge J, Gaspar C, Dion Y, et al. Association of intronic variants of the BTBD9 gene with Tourette syndrome. Arch Neurol. 2009 Oct;66(10):1267-72.

Rosenbloom KR, Dreszer TR, Long JC, Malladi VS, Sloan CA, Raney BJ, et al. ENCODE whole-genome data in the UCSC Genome Browser: update 2012. Nucleic Acids Res. 2012 Jan;40(Database issue):D912-7.

Royo JL, Bessa J, Hidalgo C, Fernandez-Minan A, Tena JJ, Roncero Y, et al. Identification and analysis of conserved cis-regulatory regions of the MEIS1 gene. PLoS One. 2012;7(3):e33617.

Schambra U, editor. Atlas of the prenatal mouse brain: Springer; 1992.

Schattschneider J, Bode A, Wasner G, Binder A, Deuschl G, Baron R. Idiopathic restless legs syndrome: abnormalities in central somatosensory processing. J Neurol. 2004 Aug;251(8):977-82.

Schmidauer C, Sojer M, Seppi K, Stockner H, Hogl B, Biedermann B, et al. Transcranial ultrasound shows nigral hypoechogenicity in restless legs syndrome. Ann Neurol. 2005 Oct;58(4):630-4.

Schormair B, Kemlink D, Roeske D, Eckstein G, Xiong L, Lichtner P, et al. PTPRD (protein tyrosine phosphatase receptor type delta) is associated with restless legs syndrome. Nat Genet. 2008 Aug;40(8):946-8.

Schormair B, Plag J, Kaffe M, Gross N, Czamara D, Samtleben W, et al. MEIS1 and BTBD9: genetic association with restless leg syndrome in end stage renal disease. J Med Genet. 2011 Jul;48(7):462-6.

Schreiber E, Matthias P, Muller MM, Schaffner W. Rapid detection of octamer binding proteins with 'mini-extracts', prepared from a small number of cells. Nucleic Acids Res. 1989 Aug 11;17(15):6419.

Shanmugam K, Green NC, Rambaldi I, Saragovi HU, Featherstone MS. PBX and MEIS as non-DNA-binding partners in trimeric complexes with HOX proteins. Mol Cell Biol. 1999 Nov;19(11):7577-88.

Shibahara K, Sugio K, Osaki T, Uchiumi T, Maehara Y, Kohno K, et al. Nuclear expression of the Y-box binding protein, YB-1, as a novel marker of disease progression in non-small cell lung cancer. Clin Cancer Res. 2001 Oct;7(10):3151-5.

Shibao K, Takano H, Nakayama Y, Okazaki K, Nagata N, Izumi H, et al. Enhanced coexpression of YB-1 and DNA topoisomerase II alpha genes in human colorectal carcinomas. Int J Cancer. 1999 Dec 10;83(6):732-7.

Silber MH, Richardson JW. Multiple blood donations associated with iron deficiency in patients with restless legs syndrome. Mayo Clin Proc. 2003 Jan;78(1):52-4.

Silva RM, Kuan CY, Rakic P, Burke RE. Mixed lineage kinase-c-jun N-terminal kinase signaling pathway: a new therapeutic target in Parkinson's disease. Mov Disord. 2005 Jun;20(6):653-64.

Snyder AM, Wang X, Patton SM, Arosio P, Levi S, Earley CJ, et al. Mitochondrial ferritin in the substantia nigra in restless legs syndrome. J Neuropathol Exp Neurol. 2009 Nov;68(11):1193-9.

Somel M, Guo S, Fu N, Yan Z, Hu HY, Xu Y, et al. MicroRNA, mRNA, and protein expression link development and aging in human and macaque brain. Genome Res. 2010 Sep;20(9):1207-18.

Sommer M, Bachmann CG, Liebetanz KM, Schindehutte J, Tings T, Paulus W. Pregabalin in restless legs syndrome with and without neuropathic pain. Acta Neurol Scand. 2007 May;115(5):347-50.

Staedt J, Stoppe G, Kogler A, Munz D, Riemann H, Emrich D, et al. Dopamine D2 receptor alteration in patients with periodic movements in sleep (nocturnal myoclonus). J Neural Transm Gen Sect. 1993;93(1):71-4.

Staedt J, Stoppe G, Kogler A, Riemann H, Hajak G, Munz DL, et al. Nocturnal myoclonus syndrome (periodic movements in sleep) related to central dopamine D2-receptor alteration. Eur Arch Psychiatry Clin Neurosci. 1995;245(1):8-10.

Staedt J, Stoppe G, Kogler A, Riemann H, Hajak G, Munz DL, et al. Single photon emission tomography (SPET) imaging of dopamine D2 receptors in the course of dopamine replacement therapy in patients with nocturnal myoclonus syndrome (NMS). J Neural Transm Gen Sect. 1995;99(1-3):187-93.

Stefansson H, Rye DB, Hicks A, Petursson H, Ingason A, Thorgeirsson TE, et al. A genetic risk factor for periodic limb movements in sleep. N Engl J Med. 2007 Aug 16;357(7):639-47.

Sun YM, Hoang T, Neubauer JA, Walters AS. Opioids protect against substantia nigra cell degeneration under conditions of iron deprivation: a mechanism of possible relevance to the Restless Legs Syndrome (RLS) and Parkinson's disease. J Neurol Sci. 2011 May 15;304(1-2):93-101.

Swamynathan SK, Nambiar A, Guntaka RV. Role of single-stranded DNA regions and Y-box proteins in transcriptional regulation of viral and cellular genes. Faseb J. 1998 May;12(7):515-22.

Thorsteinsdottir U, Kroon E, Jerome L, Blasi F, Sauvageau G. Defining roles for HOX and MEIS1 genes in induction of acute myeloid leukemia. Mol Cell Biol. 2001 Jan;21(1):224-34.

Torii S, Yamamoto T, Tsuchiya Y, Nishida E. ERK MAP kinase in G cell cycle progression and cancer. Cancer Sci. 2006 Aug;97(8):697-702.

Trenkwalder C, Hening WA, Montagna P, Oertel WH, Allen RP, Walters AS, et al. Treatment of restless legs syndrome: an evidence-based review and implications for clinical practice. Mov Disord. 2008 Dec 15;23(16):2267-302.

Trenkwalder C, Paulus W, Walters AS. The restless legs syndrome. Lancet Neurol. 2005 Aug;4(8):465-75.

Tribl GG, Asenbaum S, Happe S, Bonelli RM, Zeitlhofer J, Auff E. Normal striatal D2 receptor binding in idiopathic restless legs syndrome with periodic leg movements in sleep. Nucl Med Commun. 2004 Jan;25(1):55-60.

Tucker ES, Lehtinen MK, Maynard T, Zirlinger M, Dulac C, Rawson N, et al. Proliferative and transcriptional identity of distinct classes of neural precursors in the mammalian olfactory epithelium. Development. 2010 Aug 1;137(15):2471-81.

Uchiumi T, Fotovati A, Sasaguri T, Shibahara K, Shimada T, Fukuda T, et al. YB-1 is important for an early stage embryonic development: neural tube formation and cell proliferation. J Biol Chem. 2006 Dec 29;281(52):40440-9.

Uetani N, Chagnon MJ, Kennedy TE, Iwakura Y, Tremblay ML. Mammalian motoneuron axon targeting requires receptor protein tyrosine phosphatases sigma and delta. J Neurosci. 2006 May 31;26(22):5872-80.

Unrath A, Juengling FD, Schork M, Kassubek J. Cortical grey matter alterations in idiopathic restless legs syndrome: An optimized voxel-based morphometry study. Mov Disord. 2007 Sep 15;22(12):1751-6.

von Spiczak S, Whone AL, Hammers A, Asselin MC, Turkheimer F, Tings T, et al. The role of opioids in restless legs syndrome: an [11C]diprenorphine PET study. Brain. 2005 Apr;128(Pt 4):906-17.

Walters AS. Toward a better definition of the restless legs syndrome. The International Restless Legs Syndrome Study Group. Mov Disord. 1995 Sep;10(5):634-42.

Walters AS. Review of receptor agonist and antagonist studies relevant to the opiate system in restless legs syndrome. Sleep Med. 2002 Jul;3(4):301-4.

Walters AS, Hickey K, Maltzman J, Verrico T, Joseph D, Hening W, et al. A questionnaire study of 138 patients with restless legs syndrome: the 'Night-Walkers' survey. Neurology. 1996 Jan;46(1):92-5.

Walters AS, Ondo WG, Zhu W, Le W. Does the endogenous opiate system play a role in the Restless Legs Syndrome? A pilot post-mortem study. J Neurol Sci. 2009 Apr 15;279(1-2):62-5.

Walters AS, Wagner ML, Hening WA, Grasing K, Mills R, Chokroverty S, et al. Successful treatment of the idiopathic restless legs syndrome in a randomized double-blind trial of oxycodone versus placebo. Sleep. 1993 Jun;16(4):327-32.

Walters AS, Winkelmann J, Trenkwalder C, Fry JM, Kataria V, Wagner M, et al. Long-term follow-up on restless legs syndrome patients treated with opioids. Mov Disord. 2001 Nov;16(6):1105-9.

Ware JC, Blumoff R, Pittard JT. Peripheral vasoconstriction in patients with sleep related periodic leg movements. Sleep. 1988 Apr;11(2):182-6.

Weissbach A, Siegesmund K, Bruggemann N, Schmidt A, Kasten M, Pichler I, et al. Exome sequencing in a family with restless legs syndrome. Mov Disord. 2012 Nov;27(13):1686-9.

Wilkins A, Ping Q, Carpenter CL. RhoBTB2 is a substrate of the mammalian Cul3 ubiquitin ligase complex. Genes Dev. 2004 Apr 15;18(8):856-61.

Wilkinson DG, Nieto MA. Detection of messenger RNA by in situ hybridization to tissue sections and whole mounts. Methods Enzymol. 1993;225:361-73.

Wilkinson MF, Shyu AB. Multifunctional regulatory proteins that control gene expression in both the nucleus and the cytoplasm. Bioessays. 2001 Sep;23(9):775-87.

Winkelman JW, Finn L, Young T. Prevalence and correlates of restless legs syndrome symptoms in the Wisconsin Sleep Cohort. Sleep Med. 2006 Oct;7(7):545-52.

Winkelman JW, Shahar E, Sharief I, Gottlieb DJ. Association of restless legs syndrome and cardiovascular disease in the Sleep Heart Health Study. Neurology. 2008 Jan 1;70(1):35-42.

Winkelmann J, Czamara D, Schormair B, Knauf F, Schulte EC, Trenkwalder C, et al. Genome-wide association study identifies novel restless legs syndrome susceptibility loci on 2p14 and 16q12.1. PLoS Genet. 2011 Jul;7(7):e1002171.

Winkelmann J, Lichtner P, Putz B, Trenkwalder C, Hauk S, Meitinger T, et al. Evidence for further genetic locus heterogeneity and confirmation of RLS-1 in restless legs syndrome. Mov Disord. 2006 Jan;21(1):28-33.

Winkelmann J, Muller-Myhsok B, Wittchen HU, Hock B, Prager M, Pfister H, et al. Complex segregation analysis of restless legs syndrome provides evidence for an autosomal dominant mode of inheritance in early age at onset families. Ann Neurol. 2002 Sep;52(3):297-302.

Winkelmann J, Schadrack J, Wetter TC, Zieglgansberger W, Trenkwalder C. Opioid and dopamine antagonist drug challenges in untreated restless legs syndrome patients. Sleep Med. 2001 Jan;2(1):57-61.

Winkelmann J, Schormair B, Lichtner P, Ripke S, Xiong L, Jalilzadeh S, et al. Genome-wide association study of restless legs syndrome identifies common variants in three genomic regions. Nat Genet. 2007 Aug;39(8):1000-6.

Winkelmann J, Wetter TC, Collado-Seidel V, Gasser T, Dichgans M, Yassouridis A, et al. Clinical characteristics and frequency of the hereditary restless legs syndrome in a population of 300 patients. Sleep. 2000 Aug 1;23(5):597-602.

Wong L, Weadick CJ, Kuo C, Chang BS, Tropepe V. Duplicate dmbx1 genes regulate progenitor cell cycle and differentiation during zebrafish midbrain and retinal development. BMC Dev Biol. 2010;10:100.

Wu Q, Maniatis T. Large exons encoding multiple ectodomains are a characteristic feature of protocadherin genes. Proc Natl Acad Sci U S A. 2000 Mar 28;97(7):3124-9.

Xiong L, Catoire H, Dion P, Gaspar C, Lafreniere RG, Girard SL, et al. MEIS1 intronic risk haplotype associated with restless legs syndrome affects its mRNA and protein expression levels. Hum Mol Genet. 2009 Mar 15;18(6):1065-74.

Yuan SH, Qiu Z, Ghosh A. TOX3 regulates calcium-dependent transcription in neurons. Proc Natl Acad Sci U S A. 2009 Feb 24;106(8):2909-14.

Zhang Y, Miki T, Iwanaga T, Koseki Y, Okuno M, Sunaga Y, et al. Identification, tissue expression, and functional characterization of Otx3, a novel member of the Otx family. J Biol Chem. 2002 Aug 2;277(31):28065-9.

Zhao H, Zhu W, Pan T, Xie W, Zhang A, Ondo WG, et al. Spinal cord dopamine receptor expression and function in mice with 6-OHDA lesion of the A11 nucleus and dietary iron deprivation. J Neurosci Res. 2007 Apr;85(5):1065-76.

Ziegelbauer J, Shan B, Yager D, Larabell C, Hoffmann B, Tjian R. Transcription factor MIZ-1 is regulated via microtubule association. Mol Cell. 2001 Aug;8(2):339-49.

Zucconi M, Ferri R, Allen R, Baier PC, Bruni O, Chokroverty S, et al. The official World Association of Sleep Medicine (WASM) standards for recording and scoring periodic leg movements in sleep (PLMS) and wakefulness (PLMW) developed in collaboration with a task force from the International Restless Legs Syndrome Study Group (IRLSSG). Sleep Med. 2006 Mar;7(2):175-83.

8 APPENDIX

8.1 Table: LC-MS/MS table for HCNR 617

Protein Ids	Name	Description	Peptides used for quantitation	Max fold change	Highest mean condition	Lowest mean condition
ENSMUSP00000023934	Hbb-b1	hemoglobin, beta adult major chain	1	Infinity	R	NR
ENSMUSP00000024639	Mtap2	microtubule-associated protein 2	1	Infinity	R	NR
ENSMUSP00000007865	Ccdc124	coiled-coil domain containing 124	2	18.3	R	NR
ENSMUSP00000054548	Poldip3	polymerase (DNA-directed), delta interacting protein 3	2	7.9	NR	R
ENSMUSP00000029549	Tpm3	tropomyosin 3, gamma	1	7.3	R	NR
ENSMUSP00000008036	Rplp1	ribosomal protein, large, P1	1	6.0	R	NR
ENSMUSP00000133026	Ccdc72	coiled-coil domain containing 72	2	5.0	R	NR
ENSMUSP00000023718	5430421N21Rik	RIKEN cDNA 5430421N21 gene	1	5.0	NR	R
ENSMUSP00000099706	2700094K13Rik	RIKEN cDNA 2700094K13 gene	1	4.1	R	NR
ENSMUSP00000031913	Try4	trypsin 4	1	3.1	NR	R
ENSMUSP00000038964	Rbm3	RNA binding motif protein 3	1	2.8	R	NR
ENSMUSP00000030119	Aptx	aprataxin	1	2.7	NR	R
ENSMUSP00000073034	Ewsr1	Ewing sarcoma breakpoint region 1	2	2.5	R	NR
ENSMUSP00000065845	Cggbp1	CGG triplet repeat binding protein 1	2	2.4	NR	R
ENSMUSP00000023714	4732456N10Rik	RIKEN cDNA 4732456N10 gene	1	2.4	NR	R
ENSMUSP00000003777	Taf6l	TAF6-like RNA polymerase II, p300/CBP-associated factor (PCAF)-associated factor	1	2.4	R	NR
ENSMUSP00000099422	Smarce1	SWI/SNF related, matrix associated, actin dependent regulator of chromatin, subfamily e, member 1	2	2.4	NR	R
ENSMUSP00000050142	Olfr1395	olfactory receptor 1395	1	2.4	R	NR
ENSMUSP00000000804	Ddx3x	DEAD/H (Asp-Glu-Ala-Asp/His) box polypeptide 3, X-linked	2	2.3	NR	R
ENSMUSP00000020123	Tmpo	thymopoietin	1	2.3	NR	R
ENSMUSP00000132063	Nup214	nucleoporin 214	1	2.2	R	NR
ENSMUSP00000027097	**Creb1**	**cAMP responsive element binding protein 1**	**1**	**2.2**	**R**	**NR**
ENSMUSP00000021062	Ddx5	DEAD (Asp-Glu-Ala-Asp) box polypeptide 5	3	2.2	NR	R
ENSMUSP00000018887	Myh10	myosin, heavy polypeptide 10, non-muscle	3	2.2	NR	R
ENSMUSP00000061012	Hmgn1	high mobility group nucleosomal binding domain 1	2	2.1	R	NR
ENSMUSP00000006625	Rbm14	RNA binding motif protein 14	3	2.1	NR	R
ENSMUSP00000028607	Caprin1	cell cycle associated protein 1	1	2.0	NR	R
ENSMUSP00000027777	**Parp1**	**poly (ADP-ribose) polymerase family, member 1**	**18**	**2.0**	**NR**	**R**
ENSMUSP00000028672	Mdk	midkine	1	2.0	R	NR
ENSMUSP00000039110	Serbp1	serpine1 mRNA binding protein 1	8	1.9	R	NR
ENSMUSP00000075067	Npm1	nucleophosmin 1	10	1.8	R	NR
ENSMUSP00000078589	**Ybx1**	**Y box protein 1**	**2**	**1.8**	**R**	**NR**
ENSMUSP00000072556	Hmga2	high mobility group AT-hook 2	3	1.8	R	NR
ENSMUSP00000034597	Tmprss13	transmembrane protease, serine 13	1	1.8	R	NR
ENSMUSP00000120014	Nhp2	NHP2 ribonucleoprotein homolog (yeast)	2	1.7	R	NR
ENSMUSP00000055535	Ddx17	DEAD (Asp-Glu-Ala-Asp) box polypeptide 17	3	1.7	NR	R
ENSMUSP00000031910	Prss1	protease, serine, 1 (trypsin 1)	2	1.7	R	NR
ENSMUSP00000071486	Actg1	actin, gamma, cytoplasmic 1	1	1.6	R	NR
ENSMUSP00000078670	Gm10036	predicted gene 10036	2	1.6	NR	R
ENSMUSP00000101218	E230028L10Rik	RIKEN cDNA E230028L10 gene	1	1.6	NR	R
ENSMUSP00000026125	Alyref	Aly/REF export factor	5	1.6	R	NR
ENSMUSP00000015361	Hmgb3	high mobility group box 3	5	1.6	R	NR
ENSMUSP00000052642	Cirbp	cold inducible RNA binding protein	1	1.6	R	NR
ENSMUSP00000024779	Usp49	ubiquitin specific peptidase 49	1	1.6	R	NR
ENSMUSP00000030207	Psip1	PC4 and SFRS1 interacting protein 1	15	1.6	R	NR
ENSMUSP00000042691	Ddx21	DEAD (Asp-Glu-Ala-Asp) box polypeptide 21	1	1.6	NR	R
ENSMUSP00000072775	Gm8991	predicted pseudogene 8991	8	1.6	R	NR
ENSMUSP00000071166	Gm5619	predicted gene 5619	1	1.5	NR	R
ENSMUSP00000031931	2210010C04Rik	RIKEN cDNA 2210010C04 gene	2	1.5	R	NR
ENSMUSP00000006754	Ubtf	upstream binding transcription factor, RNA polymerase I	3	1.5	NR	R
ENSMUSP00000064970	Dach1	dachshund 1 (Drosophila)	1	1.5	NR	R
ENSMUSP00000036907	H2afz	H2A histone family, member Z	1	1.5	NR	R
ENSMUSP00000036869	Safb2	scaffold attachment factor B2	4	1.5	R	NR
ENSMUSP00000037613	Fbl	fibrillarin	1	1.5	R	NR
ENSMUSP00000053943	Basp1	brain abundant, membrane attached signal protein 1	6	1.5	R	NR
ENSMUSP00000090245	Marcks	myristoylated alanine rich protein kinase C substrate	1	1.5	R	NR
ENSMUSP00000044395	Hist1h1d	histone cluster 1, H1d	1	1.5	NR	R
ENSMUSP00000030623	Sfpq	splicing factor proline/glutamine rich (polypyrimidine tract binding protein associated	17	1.5	R	NR
ENSMUSP00000100863	Sarnp	SAP domain containing ribonucleoprotein	2	1.5	R	NR
ENSMUSP00000047235	2700029M09Rik	RIKEN cDNA 2700029M09 gene	1	1.5	NR	R
ENSMUSP00000019128	Hnrnpd	heterogeneous nuclear ribonucleoprotein D	4	1.5	R	NR
ENSMUSP00000065940	Hmgb2	high mobility group box 2	8	1.5	R	NR
ENSMUSP00000068896	Top2a	topoisomerase (DNA) II alpha	7	1.5	NR	R

8.2 List of figures

8.3 List of tables

9 PUBLICATIONS

1) Schormair B, Plag J, **Kaffe M**, Gross N, Czamara D, Samtleben W, Lichtner P, Ströhle A, Stefanidis I, Vainas A, Dardiotis E, Sakkas GK, Gieger C, Müller-Myhsok B, Meitinger T, Heemann U, Hadjigeorgiou GM, Oexle K, Winkelmann J

MEIS1 and BTBD9: genetic association with restless leg syndrome in end stage renal disease

J Med Genet. 2011 Jul;48(7):462-6

2) Winkelmann J, Czamara D, Schormair B, Knauf F, Schulte EC, Trenkwalder C, Dauvilliers Y, Polo O, Högl B, Berger K, Fuhs A, Gross N, Stiasny-Kolster K, Oertel W, Bachmann CG, Paulus W, Xiong L, Montplaisir J, Rouleau GA, Fietze I, Vávrová J, Kemlink D, Sonka K, Nevsimalova S, Lin SC, Wszolek Z, Vilariño-Güell C, Farrer MJ, Gschliesser V, Frauscher B, Falkenstetter T, Poewe W, Allen RP, Earley CJ, Ondo WG, Le WD, Spieler D, **Kaffe M**, Zimprich A, Kettunen J, Perola M, Silander K, Cournu-Rebeix I, Francavilla M, Fontenille C, Fontaine B, Vodicka P, Prokisch H, Lichtner P, Peppard P, Faraco J, Mignot E, Gieger C, Illig T, Wichmann HE, Müller-Myhsok B, Meitinger T

Genome-Wide Association Study Identifies Novel Restless Legs Syndrome Susceptibility Loci on 2p14 and 16q12.1

PLoS Genet. 2011 Jul;7(7):e1002171

3) Kaffe M*, Gross N*, Castrop F, Dresel C, Gieger C, Lichtner P, Haslinger B, Winkelmann J.

Mutational screening of THAP1 in a German population with primary dystonia

Parkinsonism Relat Disord. 2012 Jan;18(1):104-6

4) Derek Spieler*, **Maria Kaffe***, Franziska Knauf*,ChIP Jose Bessa, Juan Tena, Florian Giesert, Barbara Schormair, Phd Laumen, Peter Lichtner, Christian Gieger, Darina Dzamara, Bertram Müller-Myhsok, Ronald Naumann, Wolfgang Wurst, Helmut Laumen, Fernando Casares, Jose Luis Gómez-Skarmeta, Juliane Winkelmann

Restless Legs Syndrome-associated rs12469063 in MEIS1 confers altered gene expression in the embryonic ganglionic eminences

(in submission process), *shared first authorship